Atmos. Chem. Phys., 25, 73–91, 2025
https://doi.org/10.5194/acp-25-73-2025

Atmospheric Chemistry and Physics
Open Access
EGU

Significant role of biomass burning in heavy haze formation in Nanjing, a megacity in China: molecular-level insights from intensive $PM_{2.5}$ sampling on winter hazy days

Mingjie Kang[1,2], Mengying Bao[1,2,3], Wenhuai Song[1,2], Aduburexiati Abulimiti[1,2], Changliu Wu[1,2], Fang Cao[1,2], Sönke Szidat[4], and Yanlin Zhang[1,2]

[1]School of Ecology and Applied Meteorology, Nanjing University of Information Science & Technology, Nanjing, 210044, China
[2]Atmospheric Environment Center, Joint Laboratory for International Cooperation on Climate and Environmental Change, Ministry of Education, Nanjing University of Information Science & Technology, Nanjing, 210044, China
[3]Huzhou Meteorological Administration, Huzhou, 313000, China
[4]Department of Chemistry, Biochemistry and Pharmaceutical Sciences and Oeschger Centre for Climate Change Research, University of Bern, Bern, 3012, Switzerland

Correspondence: Yanlin Zhang (dryanlinzhang@outlook.com, zhangyanlin@nuist.edu.cn)

Received: 7 July 2024 – Discussion started: 19 August 2024
Revised: 17 October 2024 – Accepted: 28 October 2024 – Published: 7 January 2025

Abstract. Reports on the molecular-level characterization of primary and secondary constituents in $PM_{2.5}$ at high temporal resolution, particularly during haze events, are still limited. This study employed comprehensive analytical methods to examine the molecular composition and source contributions of $PM_{2.5}$, with samples collected approximately every 2 h during hazy winter days. Results show that organic matter was the predominant species, followed by nitrate (NO_3^-). Radiocarbon analysis of carbonaceous fractions reveals that fossil fuels account for 61 %–82 % of water-soluble organic carbon (WSOC), likely resulting from increased fossil fuel consumption during cold heating months. Interestingly, the contribution of non-fossil sources to WSOC enhanced with worsening haze pollution, coinciding with significantly intensified biomass burning (BB). BB was identified as the largest contributor to organic carbon (OC) in both concentration and proportion, due to intensive BB emissions in the surrounding areas, especially on heavily polluted days. For secondary sources, naphthalene-derived secondary organic carbon (SOC) contributed more to OC in $PM_{2.5}$ (0.27 %–2.46 %) compared to biogenic SOC (0.05 %–1.10 %), suggesting anthropogenic volatile organic compounds (VOCs), such as those from fossil fuel and biomass combustion, play a major role in SOC formation in urban aerosols during winter. In addition to promoting secondary aerosol formation, BB could also enhance emissions from other sources, as evidenced by significant correlations between BB tracers and various other source tracers. These findings highlight the significant role of BB in contributing to heavy winter haze.

Published by Copernicus Publications on behalf of the European Geosciences Union.

1 Introduction

The air quality of China has significantly improved over the past decade due to widespread implementation of emission controls. However, this progress was unexpectedly disrupted by severe air pollution during the COVID-19 lockdown, when anthropogenic emissions dropped dramatically (Huang et al., 2020b; Le et al., 2020; Wang et al., 2020). This highlights the persistent challenge of controlling $PM_{2.5}$ pollution, especially during cold seasons in megacities. Moreover, the emergence of ozone (O_3) pollution in many urban areas complicates the situation. Rising O_3 levels, associated with increased atmospheric oxidation capacity (Kang et al., 2021), lead to more complex air pollution scenarios due to intricate secondary aerosol formations and the combined effects of $PM_{2.5}$ and O_3.

$PM_{2.5}$ affects air visibility, the regional and global radiation balance, the hydrological cycle (Kaufman et al., 2002), and both human and ecosystem health (Alexeeff et al., 2023; Chen et al., 2022; Pope et al., 2004; Wang et al., 2022). In response, scientists have conducted numerous studies to analyze aerosol components and emission sources (Cheng et al., 2016; Huang et al., 2014, 2020b, a; Jimenez et al., 2009; Kang et al., 2016, 2018a, b, 2019; Li et al., 2016a; Liu et al., 2014; Sun et al., 2014; Wang et al., 2006; Yang et al., 2024; Zhang et al., 2012, 2018). These studies indicate that $PM_{2.5}$ pollution results from the interplay between primary and secondary sources, encompassing both anthropogenic and biogenic origins. Primary sources include plant emissions, fungal spores, soil dust, fossil fuel combustion, and biomass burning (BB) (Anon, 2002; Fu et al., 2012; Kang et al., 2018b, a; Morris et al., 2011; Pöschl et al., 2010; Simoneit, 2002; Zhang et al., 2015, 2016). Secondary sources primarily involve the homogeneous and heterogeneous reactions of biogenic and anthropogenic precursors (e.g., NO_x, NH_3, SO_2, and volatile organic compounds (VOCs)) (Fu et al., 2010; Huang et al., 2014). Many $PM_{2.5}$ species contain origin information and can therefore serve as tracers to identify specific sources.

For example, saccharides, including anhydrosugars, sugars, and sugar alcohols, are important water-soluble organic constituents of aerosols (Simoneit et al., 2004b; Sindelarova et al., 2014). These compounds can act as a cloud condensation nucleus and ice nuclei, thus influencing Earth's climate and water supply (Kaufman et al., 2002). Among them, levoglucosan is widely used as a typical tracer for BB (Elias et al., 2001; Li et al., 2021b; Liu et al., 2013). BB has a substantial impact on the secondary organic aerosol (SOA) budget and climate change (Chen et al., 2017b; Zhang et al., 2024). For instance, substituted phenols from lignin combustion, which also serve as BB tracers, undergo aqueous-phase oxidation with photooxidants to form SOA, significantly influencing the evolution of organic aerosols (Zhang et al., 2024). However, the contribution of BB emissions to SOA formation is not yet well understood, leading to inaccurate representation in regional and global atmospheric chemistry models. Molecular-level studies of the relationship between BB tracers and SOA tracers at high temporal resolution can provide valuable insights into this issue. Sugar alcohols, such as arabitol and mannitol, can be used to assess the contribution of airborne fungal spores to carbonaceous aerosols (Bauer et al., 2008a, b; Fu et al., 2012, 2016). Additionally, primary sugars like glucose are useful markers for plant pollen, fruits, and detritus (Fu et al., 2016; Puxbaum and Tenze-Kunit, 2003).

SOAs are also a significant fraction of atmospheric aerosols, formed through the reactions of oxidants (e.g., OH) with both biogenic and anthropogenic VOCs (Claeys et al., 2004; Hallquist et al., 2009; Huang et al., 2014; Mozaffar et al., 2020). Biogenic VOCs, such as isoprene, monoterpenes, and sesquiterpenes, play a crucial role in global SOA formation and atmospheric processes (Claeys et al., 2004; Griffin et al., 1999; Guenther et al., 2006; Pöschl et al., 2010; Sindelarova et al., 2014; Zhang et al., 2007). In contrast, anthropogenic VOCs (e.g., aromatic hydrocarbons) are more prevalent in urban areas where coal combustion, transportation, solvent use, and biofuel/biomass burning contribute significantly (Chen et al., 2017b; Ding et al., 2017; Srivastava et al., 2022). Despite their importance, comprehensive characterization of SOA at the molecular level is challenging due to complex formation processes and fluctuating meteorological conditions. The lack of detailed molecular-level information regarding the composition, abundance, and formation mechanisms of SOA at high temporal resolution introduces uncertainties in modeling and forecasting of air pollutants (Zhang et al., 2022, 2023). As a result, accurately simulating SOA with chemical transport models becomes increasingly difficult.

In addition to the organic species mentioned above, secondary inorganic aerosol (SIA), which includes sulfate (SO_4^{2-}), nitrate (NO_3^-), and ammonium (NH_4^+), also constitutes a significant portion of fine aerosols, particularly on heavily polluted days (Fu et al., 2012; Huang et al., 2014; Lu et al., 2019; Yan et al., 2023). Nitrate and sulfate in $PM_{2.5}$ are primarily formed through secondary processes and are expected to have substantial regional impacts upon emission, especially in winter. A recent study reported that nitrate made up the largest fraction of $PM_{2.5}$ in China during severe haze events, and reducing NO_x emissions was considered an effective strategy for combating air pollution (Yan et al., 2023). However, this conclusion was called into question by the persistent severe haze during the COVID-19 lockdown, when NO_x emissions significantly declined (Le et al., 2020), suggesting the complexity of $PM_{2.5}$ pollution and the need for further research.

Although previous studies have provided valuable insights into aerosol components, the molecular-level compositions and concentrations of fine particles remain poorly understood due to their high spatial and temporal variability, especially at sub-daily (hourly) levels. One reason for this gap is that

aerosol properties can change during transport through dry or wet deposition, in-cloud processes, and atmospheric chemical reactions. Therefore, intensive aerosol sampling at high temporal resolution is essential for accurately quantifying $PM_{2.5}$ components and their source contributions. Most prior studies have focused on comparing hazy and clean days, with few studies examining variations among different hazy days on a sub-daily basis, partly due to the challenges associated with frequent aerosol sampling. However, such molecular-level data at high temporal resolution are crucial for identifying the key factors that control haze formation, which is vital for developing regulatory standards that can adapt to rapid changes in aerosol composition and concentrations over time and across areas. Furthermore, the impacts of aerosol particles with varying properties (e.g., chemical composition) on climate (Kanakidou et al., 2005; Kawana et al., 2022) remain unclear. Obtaining molecular-level $PM_{2.5}$ data at hourly intervals would greatly enhance our understanding of these issues.

In this study, we systematically unraveled the hourly variation in molecular-level $PM_{2.5}$ components during haze events in Nanjing, a major city in the Yangtze River Delta with active industries and a dense population. Concentrations of key organic and inorganic components, such as BB tracers, sugar and sugar alcohols, oxidation products (e.g., biogenic SOA tracers and aromatic acids), and water-soluble icons, were measured and compared across three different haze pollution levels. Contributions of primary sources to organic carbon (OC) in $PM_{2.5}$ samples, including BB, fungal spores, and plant debris, were estimated. Additionally, we calculated the contributions of secondary OC formed from biogenic and anthropogenic VOCs to the total OC. Radiocarbon measurements were performed on water-soluble organic carbon (WSOC) to accurately assess the contributions of fossil and non-fossil sources. Molecular-level results on $PM_{2.5}$ components and source contributions at high temporal resolution will help understand haze formation and evolution in megacities.

2 Materials and methods

2.1 Sampling

The sampling site was situated on the rooftop of a building at the Nanjing University of Information Science and Technology in Nanjing, China (32.2° N, 118.72° E). A total of 23 $PM_{2.5}$ samples were collected on prebaked quartz fiber filters (Pallflex) at approximately 2 h intervals from 31 December 2017 to 2 January 2018. A high-volume air sampler (KC-1000, Qingdao Laoshan Electric Inc., China) was used, operating at a flow rate of 1.05 $m^3\ min^{-1}$. Field blanks were also collected with the pump off during sampling. All samples were stored in darkness at −20 °C for later analysis. The entire sampling period was divided into three episodes based on $PM_{2.5}$ levels: > 200, 100–200, and < 100 $\mu g\ m^{-3}$, reflecting a transition from heavily polluted to moderately polluted days.

2.2 Measurements of organic molecules

Sugar compounds, including anhydrosugars, sugar alcohols, and sugars, were measured using ion chromatography (Dionex ICS-5000+, ThermoFisher Scientific, USA) after extraction with ultra-pure water (Milli-Q Reference, USA). Standard curve establishment and blank corrections were performed during the analysis. Other organic compounds, such as biogenic SOA tracers (isoprene, sesquiterpene, and monoterpene) and other significant organic molecules, were determined using gas chromatography/mass spectrometry (Agilent Technologies, Santa Clara, CA). Average recoveries ranged from 70 % to 110 %, and repeatability tests showed deviations of less than 15 %. All data were corrected with field blanks. Further details on measurements can be found in previous studies (Bao et al., 2023). The total mass concentrations of SOC produced by isoprene (using 2-methylglyceric acid and 2-methyltetrols), α-/β-pinene, and β-caryophyllene were estimated using the tracer-based method by Kleindienst et al. (2007). BB-derived OC and fungal-spore-derived OC were calculated using methods from earlier reports (Bauer et al., 2008a; Fu et al., 2014).

2.3 Measurements of OC, EC, WSOC, and inorganic icons

The elemental and organic carbon content was measured using a Sunset Laboratory EC/OC analyzer with the Interagency Monitoring of Protected Visual Environments (IMPROVE) seven-step heating method, which has been shown to provide more accurate measurements of EC and OC (Wu et al., 2020). Details regarding the determination of WSOC can be found in Bao et al. (2022). Water-soluble ions were analyzed using ion chromatography (IC), with further information available in Bao et al. (2023). The detected inorganic icons are listed in Table 1.

2.4 ^{14}C analysis of the carbonaceous fractions

The ^{14}C content of WSOC was determined by extracting WSOC with deionized water and then collecting the extracted solution for ^{14}C measurement using chemical wet oxidation of the eluate (Song et al., 2022). The ^{14}C results are expressed as fractions of measured carbon, calculated as follows ($F^{14}C$):

$$F^{14}C = \frac{\left(^{14}C/^{12}C\right)_{sample}}{\left(^{14}C/^{12}C\right)_{1950}}, \quad (1)$$

where $\left(^{14}C/^{12}C\right)_{1950}$ is the reference isotopic ratio from 1950. The $F^{14}C$ values were then corrected by dividing by the reference value ($f_{nf,ref}$) to remove potential impacts of

Table 1. Concentrations of key $PM_{2.5}$ components in aerosol samples collected during winter pollution episodes in urban Nanjing.

$PM_{2.5}$ ($\mu g\,m^{-3}$)	> 200				100–200				< 100			
Species	Mean	SD	Min	Max	Mean	SD	Min	Max	Mean	SD	Min	Max
EC ($\mu g\,m^{-3}$)	2.67	0.26	2.27	3.08	2.00	0.08	1.93	2.14	1.73	0.31	1.26	2.24
OC ($\mu g\,m^{-3}$)	35.4	4.78	23.8	41.1	23.7	3.86	18.5	28.7	15.3	6.19	8.74	26.7
TC ($\mu g\,m^{-3}$)	38.1	4.85	26.0	43.4	25.7	3.91	20.5	30.7	17.0	6.39	10.2	28.8
WSOC ($\mu g\,m^{-3}$)	14.3	2.62	8.97	18.1	10.2	1.30	8.11	11.4	6.21	1.90	3.84	8.26
WISOC ($\mu g\,m^{-3}$)	21.1	3.68	14.8	25.8	13.5	2.78	10.4	17.5	9.87	4.64	4.55	19.4
OC/EC	13.3	2.08	10.5	17.4	11.8	1.74	9.57	14.4	8.70	2.72	6.00	13.2
WSOC/OC	0.40	0.06	0.31	0.49	0.43	0.03	0.39	0.47	0.35	0.17	nd	0.51
WISOC/OC	0.60	0.06	0.51	0.69	0.57	0.03	0.53	0.61	0.65	0.17	0.49	1.00
14C-WSOC	0.31	0.06	0.25	0.39	0.25	0.02	0.23	0.28	0.24	0.04	0.18	0.29
Inorganic icons ($\mu g\,m^{-3}$)												
F^-	0.08	0.03	0.05	0.12	0.16	0.20	0.06	0.52	0.05	0.02	0.02	0.08
Cl^-	7.00	1.66	3.86	10.2	6.51	1.50	4.26	7.86	5.51	2.62	1.88	10.2
NO_3^-	56.0	4.39	48.7	62.4	33.9	6.50	24.0	40.1	12.7	4.37	5.75	17.7
SO_4^{2-}	30.9	4.42	26.4	38.8	19.1	3.78	13.2	23.8	10.4	3.95	6.59	19.4
NH_4^+	28.0	3.20	20.3	30.9	17.1	3.60	10.8	19.7	8.52	2.35	4.97	11.4
PO_4^{3-}	0.14	0.02	0.11	0.17	0.07	0.03	0.03	0.12	0.02	0.01	0.01	0.03
Na^+	0.73	0.15	0.47	0.98	0.83	0.18	0.59	1.08	0.47	0.16	0.29	0.76
Ca^{2+}	0.73	0.41	0.35	1.58	1.23	0.55	0.76	1.99	0.40	0.16	0.19	0.62
nss-Ca^{2+}	0.70	0.41	0.32	1.55	1.20	0.55	0.73	1.96	0.38	0.16	0.17	0.61
K^+	0.98	0.24	0.72	1.52	1.01	0.34	0.62	1.40	0.65	0.48	0.22	1.69
nss-K^+	0.95	0.24	0.69	1.49	0.98	0.34	0.60	1.36	0.64	0.48	0.21	1.67
Mg^{2+}	0.69	0.37	0.25	1.18	0.24	0.14	0.10	0.42	0.10	0.07	0.03	0.22
Anhydrosugars ($ng\,m^{-3}$)												
Levoglucosan (L)	471	122	284	721	185	28.1	142	219	201	121	59.0	395
Galactosan (G)	39.6	19.1	4.84	63.6	73.2	14.8	55.1	94.1	51.0	44.6	6.70	115
Mannosan (M)	45.4	21.2	20.8	81.9	14.8	9.73	4.79	30.3	14.0	8.11	6.63	25.4
L/M	11.5	3.21	5.86	16.5	18.3	12.4	4.67	38.0	22.4	12.7	8.88	38.2
M/G	2.86	4.83	0.41	15.6	0.20	0.13	0.07	0.41	0.66	1.20	nd	3.09
L/K^+	0.51	0.19	0.21	0.76	0.20	0.07	0.14	0.29	0.44	0.33	0.06	1.04
Sugar alcohol ($ng\,m^{-3}$)												
Arabitol	30.5	10.3	12.0	44.1	28.8	10.4	16.6	42.1	17.8	13.4	4.59	48.2
Mannitol	14.4	6.24	0.47	24.4	14.2	4.12	7.92	18.4	12.9	7.20	2.43	22.0
Glycerol	295	151	119	561	1822	1916	376	4062	2348	1334	652	4749
Sugars ($ng\,m^{-3}$)												
Trehalose	851	874	86.5	2970	1057	1112	302	3023	672	521	257	1378
Glucose	203	85.1	49.3	377	312	148	193	551	158	56.0	69.8	240
Total measured saccharides	1951	896	633	3841	3507	1632	1738	4976	3474	1238	1478	5436
Isoprene SOA tracers ($ng\,m^{-3}$)												
Cis-2-methyl-1,3,4-trihydroxy-1-butene	0.38	0.42	0.02	1.26	0.62	0.17	0.38	0.85	0.36	0.17	0.11	0.68
3-Methyl-2,3,4-trihydroxy-1-butene	0.45	0.67	0.03	2.17	0.59	0.24	0.26	0.93	0.64	0.37	0.01	1.07
Trans-2-methyl-1,3,4-trihydroxy-1-butene	0.76	0.83	0.03	2.87	0.99	0.53	0.41	1.81	0.74	0.52	0.06	1.55
Sum of C5-alkene triols	1.59	1.83	0.07	6.30	2.20	0.56	1.66	2.91	1.74	0.99	0.18	3.19
2-Methylthreitol	0.69	1.16	0.07	3.78	1.52	0.60	0.65	2.26	1.16	0.92	0.03	3.11
2-Methylerythritol	1.17	1.55	0.10	4.93	2.30	0.69	1.29	2.97	2.10	1.19	0.41	4.30
Sum of 2-methyltetrols	1.86	2.68	0.20	8.71	3.81	1.20	1.94	4.67	3.26	2.09	0.45	7.41
2-Methylglyceric acid	2.05	1.86	0.21	5.93	2.56	0.96	1.13	3.52	1.58	1.09	0.35	3.80
Sum of isoprene SOA	5.51	6.23	0.56	20.9	8.58	2.52	4.80	11.1	6.58	4.10	0.97	14.4

Table 1. Continued.

$PM_{2.5}$ ($\mu g\,m^{-3}$)	> 200				100–200				< 100			
Species	Mean	SD	Min	Max	Mean	SD	Min	Max	Mean	SD	Min	Max
Monoterpene SOA tracers ($ng\,m^{-3}$)												
3-Hydroxyglutaric acid (3-HGA)	2.45	1.64	0.94	5.52	2.75	2.30	1.02	6.60	0.95	0.39	0.42	1.53
Pinonic	1.61	2.15	0.05	6.91	3.41	1.67	1.65	5.64	1.04	0.57	0.38	1.81
Pinic	0.32	0.31	0.05	1.06	0.87	0.62	0.24	1.81	0.84	0.69	0.04	1.69
Sum of monoterpene SOA	4.38	4.00	1.17	13.5	7.03	3.79	3.22	12.7	2.82	0.90	1.36	4.09
Sesquiterpene SOA tracers ($ng\,m^{-3}$)												
β-Caryophylinic acid	0.26	0.38	nd	1.03	0.22	0.42	nd	0.97	0.29	0.45	nd	1.33
Total measured biogenic SOA tracers	10.2	10.2	1.80	34.7	15.8	5.75	8.14	24.3	9.69	4.92	2.36	18.6
Aromatic acids ($ng\,m^{-3}$)												
Phthalic acid (Ph)	8.02	3.05	3.00	12.4	10.5	1.77	8.09	12.8	5.88	3.73	1.45	13.0
Isophthalic acid (iPh)	10.1	5.28	0.98	21.2	11.7	6.50	6.75	20.2	5.76	3.32	1.72	11.2
Benzoic acid	5.46	2.76	0.47	11.4	5.88	0.52	5.01	6.29	4.47	2.44	1.07	8.41
Sum of aromatic acids	23.6	10.2	8.30	45.1	28.1	8.24	21.1	39.3	16.1	8.86	4.25	30.3
Hydroxyl- and polyacids ($ng\,m^{-3}$)												
Glyceric acid	2.20	1.81	0.22	6.56	3.52	1.34	2.00	4.89	2.68	1.48	0.60	5.17
Malic acid	3.00	1.45	0.95	5.73	4.32	2.06	1.52	6.60	3.67	1.88	0.77	6.51
Tartaric acid	0.45	0.54	0.06	1.89	1.10	0.42	0.49	1.48	1.37	0.83	0.14	2.83
Sum of hydroxyl and polyacids	5.66	2.63	1.24	10.4	8.94	3.73	4.01	12.2	7.73	4.14	1.51	14.5
Lignin and resin acids ($ng\,m^{-3}$)												
4-Hydroxybenzoic acid (4-HBA)	2.10	2.89	0.36	9.32	2.50	0.86	1.09	3.31	3.40	2.26	0.05	6.02
Vanillic acid	1.12	2.05	0.00	5.96	2.50	0.98	1.23	3.53	4.76	3.36	0.02	8.98
Syringic acid	28.0	40.7	0.23	97.8	0.21	0.20	0.01	0.54	1.18	2.95	0.01	8.47
Dehydroabietic acid	15.3	4.80	4.30	22.7	14.4	7.91	8.22	23.4	17.0	14.0	5.45	40.9
Sum of lignin and resin acids	46.5	38.0	15.8	114	19.7	8.78	10.8	29.5	26.3	15.6	9.58	56.1

OC – organic carbon, TC – total carbon, WSOC – water-soluble OC, WISOC – water-insoluble OC. Water-insoluble OC (WISOC) was calculated as the difference between OC and WSOC. nss-Ca^{2+} refers to non-sea-salt Ca^{2+}. Not detected – nd.

nuclear bomb tests in the 1950s and 1960s, thereby obtaining the non-fossil fractions of WSOC. More details can be found in the papers by Song et al. (2022) and Zhang et al. (2017).

$$f_{nf} = F^{14}C / f_{nf,ref} \quad (2)$$

2.5 Backward trajectories below 500 m above ground level

Regional transport also significantly influences $PM_{2.5}$ levels (Chang et al., 2019; Chen et al., 2017a). To estimate the impacts of air pollution transport on haze formation, we employed the Hybrid Single-Particle Lagrangian Integrated Trajectory (HYSPLIT) model to compute backward trajectories of air masses arriving at the sampling site (available at https://www.ready.noaa.gov/hypub-bin/trajtype.pl?runtype=archive, last access: 9 September 2024). MODIS active fire/hotspot products were utilized to evaluate the impact of open BB throughout the sampling period. The backward-trajectory analysis revealed that air masses during the sampling period were significantly influenced by BB, as illustrated in Fig. S1 in the Supplement. By comparison, the third episode demonstrated a greater influx of clean ocean air masses (Fig. S1c).

3 Results and discussion

3.1 Inorganic icons

Table 1 presents the concentrations of identified inorganic icons, with Cl^-, NO_3^-, SO_4^{2-}, and NH_4^+ being the major inorganic components throughout the sampling period. The contribution of SIA to total $PM_{2.5}$ far exceeded that of organic matter (OM) during all haze episodes, indicating SIA contributes greatly to the occurrence of heavy haze. As illustrated in Fig. 1, NO_3^- (mean: 20.1 %–25.6 %) was the second-most dominant species in $PM_{2.5}$ after OM, particularly during the heaviest haze event, which aligns with findings from a megacity in Canada (Rivellini et al., 2024). However, these percentages are higher than those reported for other megacities by Huang et al. (2014) (7.1 %–13.6 %), likely due to the spatial and temporal variations in energy mix and meteorological conditions over the years. The predominance of NO_3^- in SIA (30 %–52 %) is in agreement with the study on ni-

trate aerosols in Beijing, another megacity in China (~ 43 %) (Fan et al., 2020). Major sources of NO_3^- include vehicles, coal combustion, natural gas burning, and biomass burning (Fan et al., 2023; Lin et al., 2024; Zhang et al., 2014a). The rising levels of NO_3^- relative to SO_4^{2-} may be associated with recent declines in SO_2 emissions and increases in NH_3 emissions, which allow more HNO_3 to condense into particulate NO_3^- (Shah et al., 2024). This is supported by the strong correlation between NO_3^- and NH_4^+ ($r = 0.98$, $p < 0.01$). The highest concentration of NO_3^- ($56.0 \pm 4.4\,\mu g\,m^{-3}$) and its contribution (~ 25.6 %) occurred during the highest-$PM_{2.5}$ episode, likely linked to high relative humidity (RH) during this time (Fig. S2), which usually comes with high aerosol liquid water content (Bian et al., 2014) and accordingly promotes more heterogeneous reactions of nitrate formation (Lin et al., 2020). On the other hand, cooler temperatures during the heavy haze episode favor the partitioning of HNO_3 from the gas phase into the particulate phase. NO_3^- also showed a significant correlation with non-sea-salt SO_4^{2-} (nss-SO_4^{2-}) ($r = 0.92$, $p < 0.01$), calculated by subtracting sea-salt sulfate from total sulfate using the typical sulfate-to-sodium mass ratio of 0.252 in seawater (Yang et al., 2015), suggesting similar sources or formation pathways (Zhang et al., 2014a). In fact, under polluted conditions with high RH, reactive nitrogen chemistry in aerosol water contributes to SO_4^{2-} formation, where NO_x acts both as a precursor for nitrate and as an important oxidant for sulfate (Cheng et al., 2016). Consequently, NO_x emission reductions have great potential for simultaneously decreasing atmospheric sulfate, nitrate, and even O_3 pollution (Kang et al., 2021; Shah et al., 2024). Interestingly, the three SIA components (NO_3^-, SO_4^2, and NH_4^+) were found to have strong correlations with BB tracers (e.g., levoglucosan and mannosan), with $p < 0.01$ and r values ranging from 0.63 to 0.80. This indicates BB significantly enhances the secondary production of SIA. Given that the precursors of NO_3^- and SO_4^{2-}, NO_x and SO_2, are mainly contributed by fossil fuel combustion (e.g., transportation and industrial activities) in urban areas, these relationships suggest that BB plays a substantial role in the secondary transformation of fossil-fuel-derived precursors.

3.2 OC, EC, WSOC, and ^{14}C of WSOC

Similarly, the abundance of EC, OC, WSOC, and WISOC decreased with decreasing $PM_{2.5}$ levels, in line with growing wind speeds. In comparison to other episodes, the first episode, in which $PM_{2.5}$ levels exceeded $200\,\mu g\,m^{-3}$, exhibited relatively high RH, low temperatures, and low wind speeds (Fig. S2), demonstrating that adverse meteorological conditions can boost haze formation. As displayed in Table 1, the mass concentrations of OC and EC were in the range of 8.74–41.1 and 1.26–3.08 $\mu g\,m^{-3}$, respectively. These OC values are similar to previous reports for $PM_{2.5}$ in Nanjing, while EC levels are lower (Li et al., 2015, 2016b), reflecting a reduction in primary emissions due to stricter emission controls in recent years. There is a significant correlation between OC and EC ($r = 0.87$, $p < 0.01$, Fig. S3), suggesting they share common sources, such as BB, vehicle exhaust, and fossil fuel combustion (Ji et al., 2019). The OC/EC ratio increased with rising $PM_{2.5}$ levels, from an average of 8.7 to 13.3 (Table 1 and Fig. 2), close to those in BB-dominated regions (Boreddy et al., 2018; Zhang et al., 2014b). BB is known to emit a higher fraction of OC than EC (Andreae and Merlet, 2001), so the high OC/EC ratios in this study indicate significant contributions from BB, particularly during heavy haze events. In addition, the high OC/EC ratios (> 2.0–2.2) suggest the presence of secondary organic aerosol (Li et al., 2016b), likely linked to BB as a significant source of oxidants (Chang et al., 2024) and an important contributor to SOA formation (Li et al., 2024; Lim et al., 2019; Yee et al., 2013).

OC can be divided into water-soluble organic carbon (WSOC), which often comprises BB-derived and aged OC, and water-insoluble organic carbon (WISOC), typically representing primary OC (Zhang et al., 2014b). As shown in Fig. 2, the concentration of WISOC (4.55–25.8 $\mu g\,m^{-3}$) is generally higher than that of WSOC, making WISOC the primary component of OC. WSOC concentration ranged from

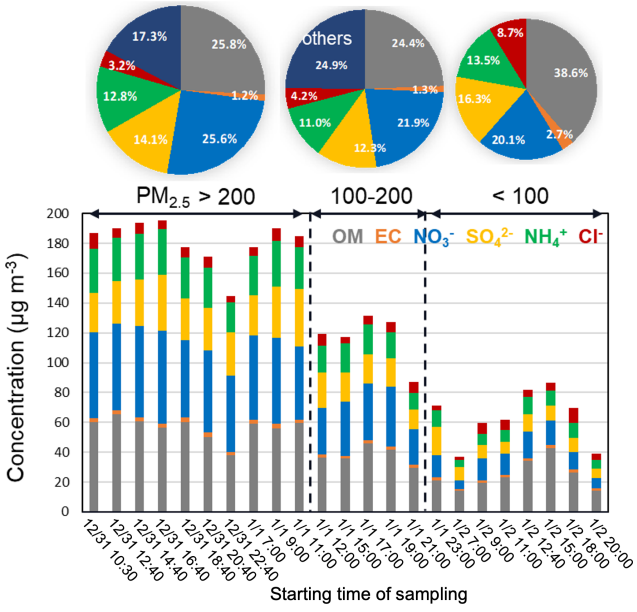

Figure 1. Temporal variations in dominant $PM_{2.5}$ compositions based on different $PM_{2.5}$ levels (< 100, 100–200, and > 200 $\mu g\,m^{-3}$). Organic matter (OM) concentrations were calculated by multiplying the OC concentration by a recommended factor of 1.6 (Turpin and Lim, 2001). "Others" refers to the remaining components of fine particles after removal of organics, secondary inorganic aerosol (sulfate, nitrate, ammonium), and chloride. The pie charts illustrate the average contribution of major components to $PM_{2.5}$ during three pollution episodes.

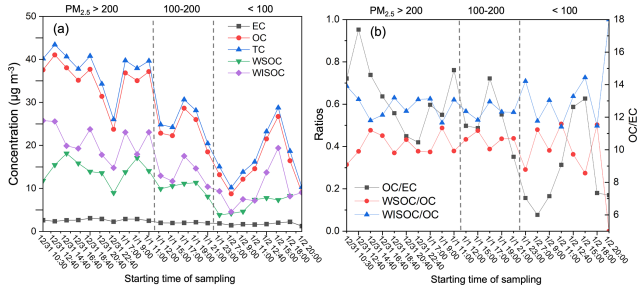

Figure 2. **(a)** Temporal variations in organic carbon (OC), elemental carbon (EC), water-soluble organic carbon (WSOC), water-insoluble organic carbon (WISOC), and total carbon (TC) (unit: $\mu g\,m^{-3}$). **(b)** Ratios of OC/EC, WSOC/OC, and WISOC/OC in $PM_{2.5}$ samples in Nanjing.

3.84 to 18.1 $\mu g\,m^{-3}$, with peak values during the most polluted episode averaging $14.3 \pm 2.62\,\mu g\,m^{-3}$, comparable to previously reported winter values of $14.0\,\mu g\,m^{-3}$ (Li et al., 2018). The WSOC/OC ratios were relatively higher during more polluted episodes ($PM_{2.5} > 100\,\mu g\,m^{-3}$), averaging 0.40 ± 0.06 and 0.43 ± 0.03, respectively (Table 1). Higher WSOC/OC ratios (> 0.4) indicate a significant contribution from secondary organic aerosol and aged aerosols (Boreddy et al., 2018; Ram et al., 2010). Given the high RH during the most polluted episode, the aqueous-phase oxidation of anthropogenic and/or biogenic VOCs is likely responsible for more WSOC formation during this time (Youn et al., 2013). In contrast, the lower WSOC/OC ratios (0.35 ± 0.17) in the third episode ($PM_{2.5} < 100\,\mu g\,m^{-3}$) suggest rising primary emissions containing large amounts of water-insoluble organics (e.g., lipid compounds), as indicated by higher WISOC/OC ratios (0.65 ± 0.17) during that time. WSOC exhibited a strong correlation with levoglucosan ($r = 0.74$, $p < 0.01$), highlighting BB as an important contributor to WSOC. This is further supported by significant correlations between BB tracers and water-soluble organic compounds, such as dicarboxylic acids (see details in the Supplement). Soluble organic gases from BB, such as phenols, can react with oxidants in aerosol liquid water and clouds, significantly contributing to SOA formation. Moreover, this aqueous SOA production greatly increases with increasing RH and decreasing temperature (Zhang et al., 2024). Considering the high RH and low temperatures during the most polluted episode, aqueous SOA generation from BB-derived organic gases likely plays a crucial role in heavy haze formation. Aqueous SOA generation from BB emissions has also been confirmed by multiple studies (Gilardoni et al., 2016; Li et al., 2021a, 2014; Xiao et al., 2022), emphasizing the importance of BB emissions in atmospheric oxidation processes. A recent report further indicates that intermediate VOCs from BB make a considerable contribution to SOA formation (Li et al., 2024), underscoring BB's significant role in the secondary formation of atmospheric organic aerosols.

To track the trends in fossil and non-fossil contributions to carbonaceous aerosols throughout haze development, ^{14}C measurements were applied to quantify the sources of WSOC. As presented in Table 1 and Fig. 3, the non-fossil fraction of WSOC was in the range of 18 %–39 % (mean: 26 %), indicating that fossil fuel sources were the primary contributors to WSOC on winter hazy days (61 %–82 %, mean: 74 %) (Fig. S4). These high fossil contributions align with previous observations in Beijing during haze events in winter (~ 61 %) (Zhang et al., 2017) and in spring (~ 54 %) (Liu et al., 2016). The variations in ^{14}C levels may reflect differing origins and formation processes of WSOC across regions and seasons. The substantial fossil fuel contribution in this study could be attributed to increased fossil fuel consumption for heating and coal-fired industrial activities during cold days, as well as traffic emissions near the sampling sites. Interestingly, while fossil fuels predominated, the contribution of non-fossil sources increased with haze intensity, suggesting their significant role in heavy haze formation. A similar trend was noted in northern India, where the non-fossil fraction of organic aerosols was higher during polluted cold periods compared to warmer months (Bhattu et al., 2024). Notably, the highest non-fossil percentages ($31\,\% \pm 6\,\%$) coincided with peak BB contributions during the haziest episode. This is evidenced by the relationship between non-fossil WSOC and BB markers (e.g., syringic acid, $r = 0.68$, $p < 0.01$), indicating that BB was a significant non-fossil source of WSOC and likely a key driver of severe winter haze, despite the substantial fossil fuel contribution at the site. Previous studies have also emphasized the role of aqueous-phase photochemical oxidation of organic gases from BB in haze pollution (Xiao et al., 2022; Zhang et al., 2024). The contribution of aqueous-phase SOA formation could be as significant as conventional semi-volatile SOA pathways (Zhang et al., 2024). Additionally, BB chlorine emissions can enhance oxidation capacity, further promoting secondary aerosol formation (Chang et al., 2024). This study found a positive correlation between Cl^- and levoglucosan ($r = 0.50$, $p < 0.05$), suggesting that BB contributes to Cl^- levels at this site and may influence the atmospheric chemistry in this area.

3.3 Carbonaceous components

Figure 4 displays the average concentrations of carbonaceous species in $PM_{2.5}$ across three air pollution episodes. Saturated diacids ($1.66–14.6\,\mu g\,m^{-3}$) were the dominant carbonaceous components, followed by sugars and sugar alcohols ($278–4936\,ng\,m^{-3}$) and anhydrosugars ($79.4–801\,ng\,m^{-3}$). The higher concentrations of anhydrosugars during the first episode indicate a significant impact from BB during heavy haze events. In contrast, the elevated levels of sugars and sugar alcohols in the latter two episodes are likely attributed to increased wind speeds, which facilitated the resuspension of biogenic detritus and soil microbes

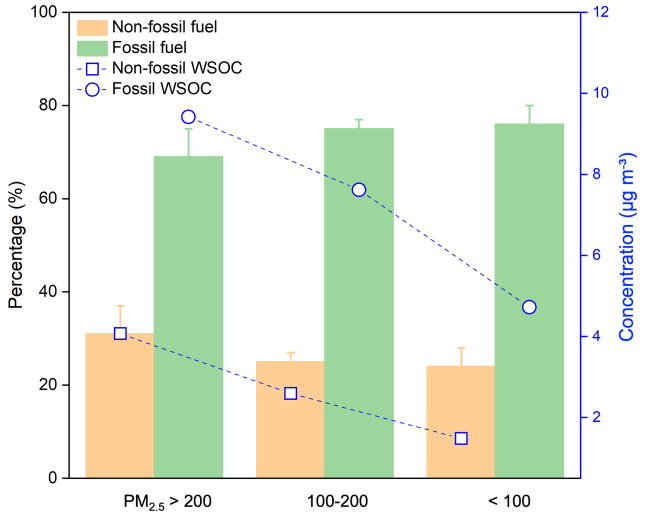

Figure 3. Comparison of fossil and non-fossil contributions to water-soluble organic carbon (WSOC) in urban $PM_{2.5}$ samples during three haze episodes (i.e., $PM_{2.5} > 200$, 100–200, and $< 100\,\mu g\,m^{-3}$).

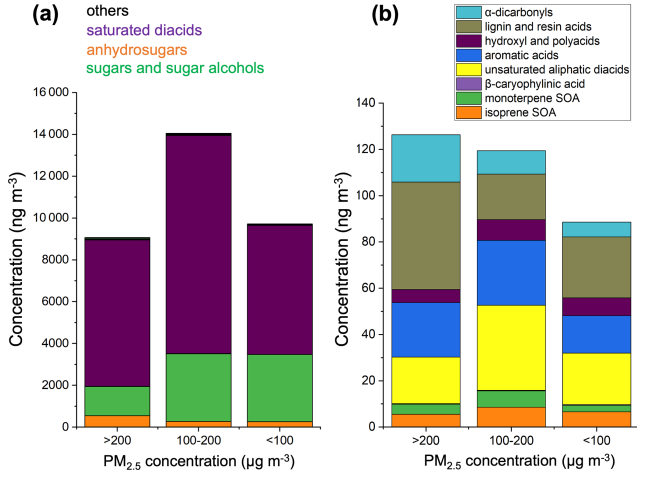

Figure 4. Average concentrations of measured carbonaceous species during three episodes with $PM_{2.5}$ levels of > 200, 100–200, and $< 100\,\mu g\,m^{-3}$. "Others" in **(a)** refers to the total of the components shown in **(b)**.

rich in these substances. Biogenic SOA tracers were relatively minor during winter haze but showed higher levels in the second episode, probably due to enhanced photooxidation under elevated temperatures and lower RH. Unsaturated aliphatic diacids and aromatic acids presented a similar trend to biogenic SOA. Additionally, lignin and resin acids – alternative tracers for BB – exhibited higher concentrations during heavy haze events, further underscoring the significance of BB in these conditions. The individual organic species identified in this study are discussed in detail below and in the Supplement.

3.3.1 Biomass burning tracers (anhydrosugars and lignin/resin acids)

Levoglucosan, a specific indicator of BB, is produced through the thermal degradation of cellulose (Simoneit, 2002). The highest concentration of levoglucosan was observed during the highest-$PM_{2.5}$ episode (average: $471 \pm 122\,ng\,m^{-3}$), highlighting the substantial role of BB in severe haze formation (Fig. S5). These levels exceed those reported in winter in Beijing (average: $361\,ng\,m^{-3}$) (Li et al., 2018) and are significantly higher than in the marine aerosols (average: $7.3\,ng\,m^{-3}$) (Kang et al., 2018a). Mannosan and galactosan, isomers of levoglucosan, serve as primary tracers for hemicellulose pyrolysis (Simoneit, 2002). During the sampling period, their concentrations remained considerably lower than the concentration of levoglucosan (Figs. S5 and S6). Notably, a significant correlation was found between mannosan and levoglucosan ($r = 0.78$, $p < 0.01$), suggesting they share similar sources at this site.

The ratios of levoglucosan to potassium (L/K^+) can be used to differentiate burnings from different biomasses (Urban et al., 2012). Both levoglucosan and K^+ are BB tracers, but this study found no significant correlation between the two. This is because in urban areas airborne potassium has other important sources, including meat cooking, waste incineration, and the resuspension of surface soil and fertilizers (Simoneit, 2002; Urban et al., 2012). The average L/K^+ ratios for the three episodes were 0.51 ± 0.19, 0.20 ± 0.07, and 0.44 ± 0.33. The lower ratios observed in the second episode may result from increased wind speeds, which facilitate the resuspension of potassium-rich surface soil and fertilizers (Urban et al., 2012). Additionally, the enhanced chemical degradation of levoglucosan at relatively high temperatures and low RH could further lower the L/K^+ ratios (Li et al., 2021b). Overall, the L/K^+ values in this study (0.06–1.04) agree well with those reported for crop and wood burning (Cheng et al., 2013; Urban et al., 2012), implying a mixed biofuel combustion, as supported by the isomeric ratios of anhydrosugars (Fig. S8).

The levoglucosan-to-OC (L/OC) and levoglucosan-to-EC (L/EC) ratios are widely used to evaluate the contribution of BB to aerosol abundance and potential degradation of levoglucosan (Mochida et al., 2010; Sullivan et al., 2008; Zhang et al., 2008). In this study, the L/OC and L/EC ratios are similar to those observed in December in Beijing (Li et al., 2018) but are higher than those for marine aerosols in winter (Zhu et al., 2015a). Higher L/OC and L/EC ratios generally occurred during heavy haze events (Fig. S7), further proving the greater contribution of BB to heavy haze formation. The overall decline in L/OC and L/EC ratios with decreasing $PM_{2.5}$ levels may indicate reduced BB activities and increased levoglucosan degradation.

Lignin and resin acids are also found in smoke aerosols from BB and serve as markers for this process (Simoneit, 2002). In this study, the total lignin and resin acids are found

in much lower amounts than anhydrosugars (Fig. 4). A total of three lignin products (4-hydroxybenzoic acid, vanillic acid, and syringic acid) and one resin product (dehydroabietic acid) were measured, with the highest concentrations occurring during the highest-$PM_{2.5}$ episode ($46.5 \pm 38.0\,ng\,m^{-3}$), further demonstrating the significant BB influence on heavy haze. These values are comparable to those in wintertime aerosols in Beijing ($47.5\,ng\,m^{-3}$) (Li et al., 2018). Among the lignin and resin acids, syringic acid was the most abundant during the heavy haze episode ($\sim 28.0\,ng\,m^{-3}$), while dehydroabietic acid was more prevalent in moderate and light haze episodes (~ 14.4 and $17.0\,ng\,m^{-3}$, respectively). Dehydroabietic acid and vanillic acid are typical tracers of conifer (softwood) burning, whereas syringic acid is more associated with hardwood smoke (Simoneit, 2002). The relatively high levels of dehydroabietic and syringic acids observed during the highest-$PM_{2.5}$ episode suggest a significant contribution from mixed wood burning on cold days, when a considerable amount of firewood was used for residential cooking and heating in nearby suburbs. Additionally, 4-hydroxybenzoic acid (4-HBA), a major tracer from the pyrolysis of non-woody vegetation such as grass and crop residue, ranged from 0.05 to $9.32\,ng\,m^{-3}$. A strong correlation between 4-HBA and vanillic acid ($r = 0.86$, $p < 0.01$) indicates their similar sources, such as mixed biofuel burning.

3.3.2 Primary sugars and sugar alcohols

Primary sugars identified in this study include trehalose and glucose, with concentrations in the range of 86.5–$3023\,ng\,m^{-3}$ and 49.3–$551\,ng\,m^{-3}$, respectively. Trehalose is particularly abundant in soils, especially in the fine mode ($PM_{2.5}$) (Jia and Fraser, 2011) and thus can serve as a potential tracer for resuspension of surface soil and unpaved road dust (Fu et al., 2012). This is supported by the similar trends observed for trehalose and non-sea-salt calcium (nss-Ca^{2+}) in the present study, as nss-Ca^{2+} is an indicator of soil dust, particularly in winter and spring (Virkkula et al., 2006). Trehalose showed a higher average concentration ($1057 \pm 1112\,ng\,m^{-3}$) during the second episode, likely triggered by increased wind speeds that facilitated the transport of trehalose from surface soil into the air. Glucose, also abundant in biologically active soils, is considered a marker for fugitive dust from cultivated land (Rogge et al., 2007). In addition, glucose is abundant in various plant tissues as well, such as pollen, fruits, developing leaves, and plant detritus (Graham et al., 2003). Both glucose and trehalose exhibited higher levels during moderate haze events, indicating enhanced primary biogenic sources during that time due to rising temperatures and wind speeds (Zhu et al., 2015b).

Sugar alcohols detected in this study consisted of arabitol, mannitol, and glycerol, with concentrations in the range of 4.59–48.2, 0.47–24.4, and 119–$4749\,ng\,m^{-3}$, respectively. Glycerol was the most abundant sugar alcohol, consistent with findings from previous studies (Kang et al., 2018b; Li et al., 2018; Ren et al., 2020). Glycerol levels increased as $PM_{2.5}$ concentrations declined (Fig. S9), peaking during the lowest-$PM_{2.5}$ episode ($\sim 2348\,ng\,m^{-3}$). This trend may be attributed to rising local temperatures during moderate and light haze events, as lower ambient temperatures tend to reduce microbial activities, such as fungal spore release. Conversely, higher concentrations of arabitol and mannitol exist in the highest-$PM_{2.5}$ episode ($> 200\,\mu g\,m^{-3}$), coinciding with intensified BB. These sugar alcohols can be emitted not only from natural sources like microbial activities and plant tissues but also significantly through thermal stripping during BB (Simoneit et al., 2004b). Moreover, BB can enhance the emissions and long-range transport of certain non-combusted organic compounds (Medeiros et al., 2006). Sugar alcohols have been linked to airborne detritus from mature leaves and would be more prevalent during leaf senescence (Graham et al., 2003; Medeiros et al., 2006). Therefore, elevated levels of arabitol and mannitol can be expected in aerosols heavily impacted by BB during winter, supported by correlations with levoglucosan ($r = 0.39$, $p = 0.06$ for arabitol; $r = 0.40$, $p = 0.06$ for mannitol). These results suggest that BB has a greater effect on arabitol and mannitol than on glycerol, indicating their primary sources in the region may differ.

3.3.3 Biogenic SOA tracers

The total levels of biogenic SOA tracers were in the range of 1.80–$34.7\,ng\,m^{-3}$, with higher concentrations in the second episode (averaging $15.8\,ng\,m^{-3}$) as shown in Fig. 4. Isoprene-derived SOA tracers accounted for a larger portion of the total biogenic SOA than combined contributions from monoterpenes and sesquiterpenes (Fig. S10). The average ratios of isoprene-to-monoterpene oxidation products for the three episodes were 1.16 ± 0.53, 1.44 ± 0.71, and 2.16 ± 0.94. These values were lower than those reported in mountain aerosols from central East China (about 4.9–6.7) (Fu et al., 2010), where large isoprene fluxes and high levels of atmospheric radicals like OH exist.

Isoprene, primarily emitted by terrestrial vegetation, is the predominant biogenic source of hydrocarbons in the atmosphere, though monoterpene emissions are universal among plants (Sharkey et al., 2008). Due to its reactive double bonds, isoprene can easily be oxidized by radicals (e.g., OH), contributing to tropospheric O_3 and SOA formation (Chameides et al., 1988; Claeys et al., 2004; Lin et al., 2013a). In this study, six isoprene SOA tracers were identified: three C5-alkene triols, two 2-methyltetrols, and one 2-methylglyceric acid (Table 1 and Figs. S11–S12). All tracers showed generally higher levels during the second episode, with average concentrations of $8.58 \pm 2.52\,ng\,m^{-3}$ for total isoprene SOA, $2.20 \pm 0.56\,ng\,m^{-3}$ for C5-alkene triols, $3.81 \pm 1.20\,ng\,m^{-3}$ for 2-methyltetrols (2-MTs), and $2.56 \pm 0.96\,ng\,m^{-3}$ for 2-methylglyceric acid (2-MGA). Analyzing the temporal variations in meteorological factors

and biogenic SOA concentrations reveals that peak levels typically occurred under relatively high temperatures and low RH, in agreement with findings from central China (Li et al., 2013). The similar variation patterns among isoprene SOA tracers suggest they may originate from common sources and undergo similar formation pathways, as evidenced by significant correlations between C5-alkene triols and 2-MTs/2-MGA ($r = 0.89$–0.90, $p < 0.01$). Among these, 2-methyltetrols were the dominant isoprene products (0.20–8.71 ng m^{-3}), in line with previous studies (Kang et al., 2018a; Li et al., 2018). Both 2-methyltetrols and C5-alkene triols result from isoprene photooxidation under low-NO_x ($NO_x = NO+NO_2$) conditions (Surratt et al., 2006, 2010), while 2-MGA is formed under high-NO_x conditions (Lin et al., 2013b; Surratt et al., 2006). The concentration ratios of C5-alkene triols to 2-methyltetrols remained relatively stable, except during the most polluted episode (Fig. S13), suggesting differing reaction processes during the heavy haze episode compared to moderate and light haze episodes. This discrepancy may arise from the chemical structure of the two species: C5-alkene triols, with their reactive double bonds, are more susceptible to oxidation. Consequently, the decreasing ratios of C5-alkene triols to 2-methyltetrols probably reflect the photochemical aging of organic aerosols over time.

Oxidation products of monoterpene include 3-hydroxyglutaric acid (3-HGA), pinonic acid, and pinic acid. Total monoterpene-derived SOA concentrations were in the range of 1.17–13.5 ng m^{-3}, with higher levels in the second episode, likely resulting from enhanced photooxidation favored by higher temperatures and lower RH. An obvious correlation was found between 3-HGA and pinonic acid ($r = 0.79$, $p < 0.01$), implying similar sources and formation pathways. Pinic acid is a minor component of monoterpene-derived SOA (0.04–1.81 ng m^{-3}), with concentrations lower than those of 3-HGA (0.42–6.60 ng m^{-3}) and pinonic acid (0.05–6.91 ng m^{-3}). Additionally, pinic acid correlated with lignin and resin acids, such as vanillic acid and 4-HBA ($r = 0.69$–0.76, $p < 0.01$), suggesting BB significantly enhances its secondary formation. This is because BB serves as both an important source of air pollutants and a contributor to oxidant production (Chang et al., 2024), which increase oxidation capacity and promote photochemistry and SOA formation. However, pinic acid did not exhibit the highest concentration during the heavy haze episode, despite the significant contribution from BB. This may be due to pinic acid undergoing further reactions at high RH, forming highly oxidized polar compounds through water addition and the opening of the dimethylcyclobutane ring (Claeys et al., 2007).

β-Caryophylinic acid is a product of the ozonolysis or photooxidation of β-caryophyllene (Jaoui et al., 2007), a major species of sesquiterpenes emitted by plants (Duhl et al., 2008). Overall, β-caryophylinic acid showed a slightly higher average concentration of 0.29 ng m^{-3} during the lowest-$PM_{2.5}$ event (< 100 µg m^{-3}).

3.3.4 Aromatic acids

Three aromatic acids, including phthalic acid, isophthalic acid, and benzoic acid, were determined in these aerosols. Total aromatic acid concentrations were higher during high-$PM_{2.5}$ episodes (> 100 µg m^{-3}), ranging from 8.3 to 45.1 ng m^{-3}. Phthalic acid (Ph) and isophthalic acid (iPh) were the predominant aromatic acids, with concentrations of 1.45–13.0 ng m^{-3} and 0.98–21.2 ng m^{-3}, respectively. Secondary photochemical reactions of polycyclic aromatic hydrocarbons (PAHs), such as naphthalene, are likely primary sources of Ph, which is recognized as a naphthalene-derived SOA tracer (Fine et al., 2004; Ren et al., 2020). Vehicle exhaust is a significant source of naphthalene in urban areas, suggesting that transportation emissions contributed to Ph levels at this site. Additional sources of naphthalene include biomass burning, industrial activities, and evaporation from naphthalene-containing products. By comparison, benzoic acid was a minor component in aromatic acids (0.47–11.4 ng m^{-3}). It can be directly emitted from vehicle exhaust or formed through the photochemical reactions of aromatic hydrocarbons such as toluene (Ho et al., 2015; Li et al., 2022; Rogge et al., 1993; Suh et al., 2003). The relationships among Ph, iPh, and benzoic acid ($r = 0.64$–0.79, $p < 0.01$) suggest they share common sources, such as fossil fuels.

3.3.5 Hydroxy-/polyacids

Polyacids are reported to be secondary photooxidation products of atmospheric organic precursors (Fu et al., 2008; Kawamura and Sakaguchi, 1999). In this study, three hydroxy-/polyacids were measured, including glyceric acid, malic acid, and tartaric acid. Malic acid (0.77–6.60 ng m^{-3}) was the major compound among the hydroxycarboxylic acids, followed by glyceric acid (0.22–6.56 ng m^{-3}), while tartaric acid was present in smaller amounts. This finding is consistent with earlier reports from the polluted East Asia/-Pacific region (Simoneit et al., 2004a). A significant correlation was observed between glyceric and tartaric acid ($r = 0.81$, $p < 0.01$), suggesting similar sources and/or formation pathways. Moreover, glyceric acid and tartaric acid were significantly correlated with isoprene ($r = 0.71$–0.93, $p < 0.01$) and monoterpene SOA tracers (e.g., 2-methyltetrols, C5-alkene triols, pinic, and pinonic acids) ($r = 0.65$–0.77, $p < 0.01$). Malic acid showed a positive correlation with glucose ($r = 0.65$, $p < 0.01$). These significant relationships indicate that hydroxy acids may be secondary oxidation products of biogenic VOCs and sugars (Simoneit et al., 2004a). Furthermore, glyceric acid exhibited clear correlations with aromatic acids such as iPh and benzoic acids ($r = 0.63$–0.71, $p < 0.01$), implying they may undergo similar atmospheric processing pathways. Glyceric and tartaric acids were also significantly correlated with 4-HBA and vanillic acid ($r = 0.58$–0.81, $p < 0.01$), indicating that BB contributes to their secondary production.

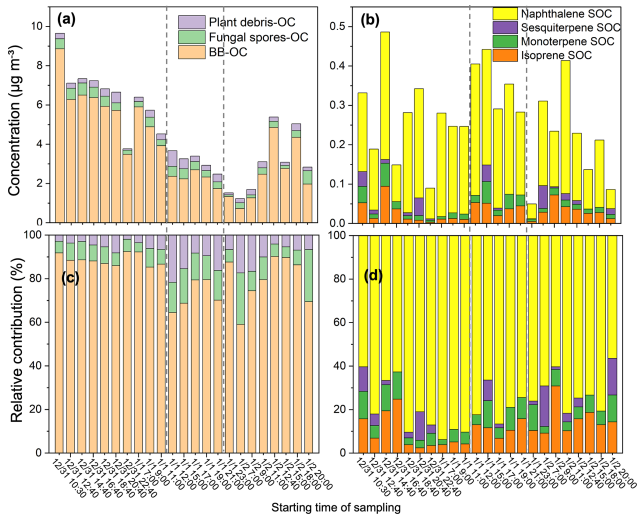

Figure 5. Concentrations of **(a)** primary OC derived from biomass burning, fungal spores, and plant debris and **(b)** secondary OC produced from isoprene, monoterpene, sesquiterpene, and naphthalene, along with their relative contributions (**c** and **d**).

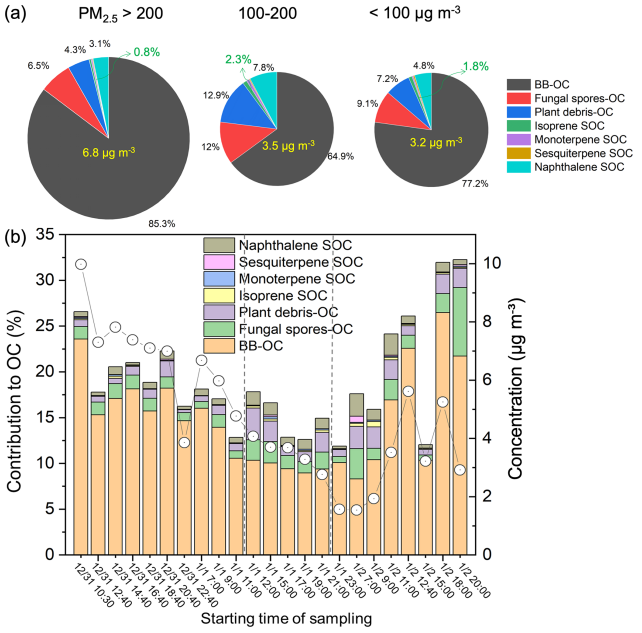

Figure 6. **(a)** Episode-averaged relative contributions of primary and secondary OC (%). The yellow numbers refer to the total tracer-based OC concentrations attributed to these sources (μg m^{-3}). The size of each pie chart is proportional to its total tracer-based OC concentration. The green arrows and numbers represent the biogenic SOC fraction contributed by isoprene, monoterpene, and sesquiterpene. **(b)** Contributions of primary and secondary OC to total OC in $PM_{2.5}$ (%), along with OC concentrations attributed to these sources (μg m^{-3}, shown as white circles).

3.4 Contributions of primary and secondary sources to OC

To evaluate the contributions of primary sources (e.g., BB, fungal spores, and plant debris) and secondary sources (e.g., oxidation reactions of PAHs and biogenic VOCs like isoprene, monoterpene, and sesquiterpene) to OC in $PM_{2.5}$, tracer-based methods were utilized. Detailed calculations and relevant conversion factors are available in our previous studies and other literature (Bauer et al., 2008a; Gelencsér et al., 2007; Holden et al., 2011; Kang et al., 2018a; Kleindienst et al., 2007, 2012; Puxbaum and Tenze-Kunit, 2003). The results are presented in Figs. 5–6 and Table 2.

Compared to other primary and secondary sources, BB made a predominant contribution to aerosol OC throughout the sampling period, in terms of both concentration (0.72–8.86 μg m^{-3}) and proportion (8.29 %–26.5 %). The most significant impact of BB occurred during the heavy haze episode, with a mean concentration of 5.79 ± 1.50 μg m^{-3} and a contribution of $16.3\,\% \pm 3.4\,\%$. This could be linked to heightened domestic wood/crop combustion for heating and cooking, as well as open BB in nearby areas, driven by lower temperatures and higher RH during this episode (Figs. S1–S2). BB chlorine emissions can elevate O_3 and OH radical levels, significantly influencing oxidation processes (Chang et al., 2024). Moreover, organic gases from BB sources can undergo gas-phase, aqueous-phase, and multiphase reactions in the atmosphere, contributing to SOA formation (Zhang et al., 2024). All these findings suggest BB's critical role in atmospheric chemistry and aerosol formation. Considering the potential atmospheric degradation of levoglucosan, BB's contribution might be somewhat underestimated, indicating that its actual fraction is likely larger. A higher BB contribution to organic aerosols during colder periods, characterized by elevated $PM_{2.5}$ concentrations, was also recently reported in northern India (Bhattu et al., 2024). The concentration of fungal-spore-derived OC was generally higher (0.44 ± 0.14 μg m^{-3}) during the highest-$PM_{2.5}$ episode, coinciding with significant BB during that time (Fig. S14). This finding aligns with earlier research that reported elevated fungal spore tracers on BB-affected days (Yang et al., 2012), indicating that BB may enhance emissions from other sources, such as fungal spores, exacerbating air pollution. However, the percentage of fungal-spore-derived OC declined with increasing $PM_{2.5}$ levels, with higher fractions noted during light haze episode ($2.38\,\% \pm 2.26\,\%$), when BB's contribution to OC remained substantial ($15.9\,\% \pm 7.01\,\%$). By comparison, OC from plant debris was higher in the second episode (0.45 ± 0.21 μg m^{-3}, $1.99\,\% \pm 1.02\,\%$), likely due to increased resuspension of surface soils and road dust resulting from elevated wind speeds and temperatures (Simoneit et al., 2004b). Overall, the total abundance of primary OC derived from BB, fungal spores, and plant debris ranged from 1.23 to 9.65 μg m^{-3}, comprising 11.3 %–31.3 % of OC, with higher concentrations in the most polluted episode (average: 6.52 ± 1.62 μg m^{-3}). Even though to-

Table 2. Concentrations of OC from primary sources (biomass burning, fungal spores, and plant debris) and SOC derived from biogenic and anthropogenic VOCs, along with their contributions to OC in $PM_{2.5}$.

$PM_{2.5}$ concentration ($\mu g\,m^{-3}$)	> 200				100–200				< 100			
	Mean	SD	Min	Max	Mean	SD	Min	Max	Mean	SD	Min	Max
Concentration ($\mu g\,m^{-3}$)												
Biomass burning OC	5.79	1.50	3.48	8.86	2.27	0.34	1.74	2.69	2.47	1.48	0.72	4.86
Fungal spores OC	0.44	0.14	0.21	0.62	0.42	0.09	0.32	0.52	0.29	0.18	0.09	0.68
Plant debris OC	0.29	0.12	0.07	0.55	0.45	0.21	0.28	0.80	0.23	0.08	0.10	0.35
Sum of primary OC	6.52	1.62	3.77	9.65	3.14	0.46	2.48	3.67	2.99	1.56	1.23	5.39
Isoprene SOC	0.03	0.03	0.003	0.09	0.04	0.01	0.02	0.05	0.03	0.02	0.01	0.07
Monoterpene SOC	0.02	0.02	0.01	0.06	0.03	0.02	0.01	0.06	0.01	0.004	0.01	0.02
Sesquiterpene SOC	0.01	0.02	0.00	0.04	0.01	0.02	0.00	0.04	0.01	0.02	0.00	0.06
Sum of biogenic SOC	0.06	0.05	0.01	0.16	0.08	0.04	0.04	0.15	0.06	0.03	0.01	0.10
Naphthalene SOC	0.21	0.08	0.08	0.32	0.27	0.05	0.21	0.33	0.15	0.10	0.04	0.34
Sum of SOC	0.26	0.11	0.09	0.49	0.36	0.07	0.28	0.44	0.21	0.12	0.05	0.41
Total	6.79	1.68	3.86	9.98	3.50	0.50	2.76	4.07	3.20	1.57	1.54	5.62
Contribution to OC (%)												
Biomass burning OC	16.3	3.39	10.6	23.6	9.63	0.56	8.96	10.3	15.9	7.01	8.29	26.5
Fungal spores OC	1.23	0.31	0.74	1.63	1.81	0.47	1.23	2.32	2.38	2.26	0.56	7.50
Plant debris OC	0.83	0.39	0.30	1.74	1.99	1.02	0.98	3.48	1.69	0.75	0.62	2.44
Sum of primary OC	18.4	3.62	12.2	25.7	13.4	1.97	11.3	16.0	19.9	8.31	11.5	31.3
Isoprene SOC	0.07	0.08	0.01	0.25	0.18	0.08	0.07	0.24	0.23	0.18	0.04	0.60
Monoterpene SOC	0.05	0.04	0.02	0.15	0.13	0.08	0.05	0.25	0.09	0.04	0.04	0.15
Sesquiterpene SOC	0.03	0.05	0.00	0.14	0.04	0.08	0.00	0.19	0.13	0.22	0.00	0.66
Sum of biogenic SOC	0.15	0.14	0.05	0.43	0.36	0.20	0.14	0.67	0.44	0.34	0.09	1.10
Naphthalene SOC	0.59	0.21	0.27	0.88	1.17	0.22	0.88	1.46	1.12	0.84	0.29	2.46
Sum of SOC	0.74	0.29	0.38	1.28	1.53	0.37	1.01	1.99	1.57	1.13	0.38	3.56
Total	19.1	3.74	12.8	26.6	15.0	2.28	12.6	17.8	21.5	8.29	11.9	32.2

tal primary OC concentrations were lower during light haze episodes ($PM_{2.5} < 100\,\mu g\,m^{-3}$), the contribution of primary OC to aerosol OC was comparable to and even exceeded (19.9 % ± 8.31 %) the contributions observed in heavy and moderate episodes.

Secondary sources, including isoprene, monoterpene, sesquiterpene, and naphthalene, contributed only 0.38 %–3.56 % of OC in $PM_{2.5}$, likely as a result of reduced photolysis during winter when sunlight is less intense. Overall, SOC showed higher levels ($0.36 \pm 0.07\,\mu g\,m^{-3}$) and contributions (1.53 % ± 0.37 %) during episodes characterized by higher temperatures and lower RH, as such weather conditions favor photochemical reactions and SOC production. Notably, naphthalene-derived SOC was the primary secondary source of OC, both in concentration (0.04–0.34 $\mu g\,m^{-3}$) and in proportion (0.27 %–2.46 %), followed by biogenic isoprene-derived SOC (0.003–0.09 $\mu g\,m^{-3}$, 0.01 %–0.60 %) (Table 2). This indicates that anthropogenic VOCs, such as those from vehicle exhaust and biomass burning, predominantly contribute to SOC in urban aerosols. Moreover, the total concentrations and fractional contributions of biogenic SOCs (0.01–0.16 $\mu g\,m^{-3}$, 0.05 %–1.10 %) were lower than those from anthropogenic sources, most likely due to significantly reduced biogenic VOC emissions and increased combustion of fossil fuels and biomass during cold winter months. The abundance and percentage of total primary and secondary OC were in the range of 1.54–9.98 $\mu g\,m^{-3}$ and 11.9 %–32.2 %, respectively, based on the tracers identified in this study. These values are comparable to those reported for winter aerosol in Beijing (6.18 %–38.3 %) (Li et al., 2018).

4 Conclusions

Molecular distributions and high temporal variations in primary and secondary components in $PM_{2.5}$ during winter hazy episodes in urban Nanjing were comprehensively characterized through intensive sampling. Our results revealed that OM dominated the total $PM_{2.5}$, followed by NO_3^-. ^{14}C analysis showed that while fossil fuel sources primarily contributed to WSOC, non-fossil sources, notably BB, became more significant as $PM_{2.5}$ pollution intensified. BB made a dominant contribution to OC due to intensive BB emissions, particularly during severe haze events. Additionally, BB-derived gases can increase oxidants and aqueous SOA formation, playing an important role in winter atmospheric chemistry. Other non-fossil sources like fungal spore emis-

sions could also be elevated by BB, whereas plant debris contributions were higher on lighter hazy days with higher wind speeds and temperatures. Overall, these findings highlight the significant role of BB in winter haze over Nanjing and underscore the need for further research into the molecular-level identification of gaseous species from BB emissions and their role in secondary aerosol formation. Additionally, although meteorological parameters have an important influence on the development of heavy haze, accurately quantifying their contribution remains a challenge for future research.

Data availability. The dataset for this paper is available upon request from the corresponding author (zhangyanlin@nuist.edu.cn).

Supplement. Information on other $PM_{2.5}$ components, including chloride, monocarboxylic acids, dicarboxylic acids, methylglyoxal, and methanesulfonic acid (MSA), is provided here, with their concentrations presented in Table S1. The HYSPLIT backward trajectories initiated over Nanjing are demonstrated in Fig. S1. The time series of meteorological parameters are shown in Fig. S2. The relationship between EC and OC in $PM_{2.5}$ is indicated in Fig. S3. Temporal variations in fossil and non-fossil contributions to WSOC are shown Fig. S4. Temporal variations in biomass burning tracers are demonstrated in Fig. S5. Average concentrations of anhydrosugars and lignin and resin products for the three episodes are indicated in Fig. S6. Temporal variations in ratios of L/M, L/OC, and L/EC and the average ratios during the three episodes are in Fig. S7. Comparison of L/M and M/G ratios between literature values and aerosols from this study is done in Fig. S8. Temporal variations in sugars and sugar alcohols are shown in Fig. S9. Average and temporal concentrations of biogenic SOA tracers during the three episodes are shown in Figs. S10–S12. Temporal variations in the concentration ratios of isoprene oxidation products are demonstrated in Fig. S13. Temporal variations in biomass-burning-derived OC, fungal-spore-derived OC, and plant-debris-derived OC are shown in Fig. S14. Temporal variations in the biogenic SOC derived from isoprene, monoterpene, and sesquiterpene are shown in Fig. S15. The supplement related to this article is available online at: https://doi.org/10.5194/acp-25-73-2025-supplement.

Author contributions. YLZ designed the research. MYB collected aerosol samples. MYB and WHS performed the laboratory analyses. The paper was written by MJK with editing from all co-authors.

Competing interests. The contact author has declared that none of the authors has any competing interests.

Disclaimer. Publisher's note: Copernicus Publications remains neutral with regard to jurisdictional claims made in the text, published maps, institutional affiliations, or any other geographical representation in this paper. While Copernicus Publications makes every effort to include appropriate place names, the final responsibility lies with the authors.

Financial support. This research has been supported by the National Natural Science Foundation of China (grant nos. 42325304, 42273087).

Review statement. This paper was edited by Arthur Chan and reviewed by six anonymous referees.

References

Alexeeff, S. E., Deosaransingh, K., Van Den Eeden, S., Schwartz, J., Liao, N. S., and Sidney, S.: Association of Long-term Exposure to Particulate Air Pollution With Cardiovascular Events in California, JAMA Network Open, 6, e230561, https://doi.org/10.1001/jamanetworkopen.2023.0561, 2023.

Andreae, M. O. and Merlet, P.: Emission of trace gases and aerosols from biomass burning, Global Biogeochem. Cy., 15, 955–966, https://doi.org/10.1029/2000GB001382, 2001.

Anon: Biomass burning – a review of organic tracers for smoke from incomplete combustion, Appl. Geochem., 17, 129–162, https://doi.org/10.1016/S0883-2927(01)00061-0, 2002.

Bao, M., Zhang, Y.-L., Cao, F., Lin, Y.-C., Hong, Y., Fan, M., Zhang, Y., Yang, X., and Xie, F.: Light absorption and source apportionment of water soluble humic-like substances (HULIS) in $PM_{2.5}$ at Nanjing, China, Environ. Res., 206, 112554, https://doi.org/10.1016/j.envres.2021.112554, 2022.

Bao, M., Zhang, Y.-L., Cao, F., Hong, Y., Lin, Y.-C., Yu, M., Jiang, H., Cheng, Z., Xu, R., and Yang, X.: Impact of fossil and non-fossil fuel sources on the molecular compositions of water-soluble humic-like substances in $PM_{2.5}$ at a suburban site of Yangtze River Delta, China, Atmos. Chem. Phys., 23, 8305–8324, https://doi.org/10.5194/acp-23-8305-2023, 2023.

Bauer, H., Claeys, M., Vermeylen, R., Schueller, E., Weinke, G., Berger, A., and Puxbaum, H.: Arabitol and mannitol as tracers for the quantification of airborne fungal spores, Atmos. Environ., 42, 588–593, https://doi.org/10.1016/j.atmosenv.2007.10.013, 2008a.

Bauer, H., Schueller, E., Weinke, G., Berger, A., Hitzenberger, R., Marr, I. L., and Puxbaum, H.: Significant contributions of fungal spores to the organic carbon and to the aerosol mass balance of the urban atmospheric aerosol, Atmos. Environ., 42, 5542–5549, https://doi.org/10.1016/j.atmosenv.2008.03.019, 2008b.

Bhattu, D., Tripathi, S. N., Bhowmik, H. S., Moschos, V., Lee, C. P., Rauber, M., Salazar, G., Abbaszade, G., Cui, T., Slowik, J. G., Vats, P., Mishra, S., Lalchandani, V., Satish, R., Rai, P., Casotto, R., Tobler, A., Kumar, V., Hao, Y., Qi, L., Khare, P., Manousakas, M. I., Wang, Q., Han, Y., Tian, J., Darfeuil, S., Minguillon, M. C., Hueglin, C., Conil, S., Rastogi, N., Srivastava, A. K., Ganguly, D., Bjelic, S., Canonaco, F., Schnelle-Kreis, J., Dominutti, P. A., Jaffrezo, J.-L., Szidat, S., Chen, Y., Cao, J., Baltensperger, U., Uzu, G., Daellenbach, K. R., El Haddad, I., and Prévôt, A. S. H.: Local incomplete combustion emissions define the $PM_{2.5}$ oxidative potential in Northern India, Nat. Commun., 15, 3517, https://doi.org/10.1038/s41467-024-47785-5, 2024.

Bian, Y. X., Zhao, C. S., Ma, N., Chen, J., and Xu, W. Y.: A study of aerosol liquid water content based on hygroscopicity measurements at high relative humidity in the North China Plain, Atmos. Chem. Phys., 14, 6417–6426, https://doi.org/10.5194/acp-14-6417-2014, 2014.

Boreddy, S. K. R., Haque, M. M., and Kawamura, K.: Long-term (2001–2012) trends of carbonaceous aerosols from a remote island in the western North Pacific: an outflow region of Asian pollutants, Atmos. Chem. Phys., 18, 1291–1306, https://doi.org/10.5194/acp-18-1291-2018, 2018.

Chameides, W. L., Lindsay, R. W., Richardson, J., and Kiang, C. S.: The Role of Biogenic Hydrocarbons in Urban Photochemical Smog: Atlanta as a Case Study, Science, 241, 1473–1475, https://doi.org/10.1126/science.3420404, 1988.

Chang, D., Li, Q., Wang, Z., Dai, J., Fu, X., Guo, J., Zhu, L., Pu, D., Cuevas, C. A., Fernandez, R. P., Wang, W., Ge, M., Fung, J. C. H., Lau, A. K. H., Granier, C., Brasseur, G., Pozzer, A., Saiz-Lopez, A., Song, Y., and Wang, T.: Significant chlorine emissions from biomass burning affect the long-term atmospheric chemistry in Asia, Nat. Sci. Rev., 11, nwae285, https://doi.org/10.1093/nsr/nwae285, 2024.

Chang, X., Wang, S., Zhao, B., Xing, J., Liu, X., Wei, L., Song, Y., Wu, W., Cai, S., Zheng, H., Ding, D., and Zheng, M.: Contributions of inter-city and regional transport to $PM_{2.5}$ concentrations in the Beijing-Tianjin-Hebei region and its implications on regional joint air pollution control, Sci. Total Environ., 660, 1191–1200, https://doi.org/10.1016/j.scitotenv.2018.12.474, 2019.

Chen, D., Liu, X., Lang, J., Zhou, Y., Wei, L., Wang, X., and Guo, X.: Estimating the contribution of regional transport to $PM_{2.5}$ air pollution in a rural area on the North China Plain, Sci. Total Environ., 583, 280–291, https://doi.org/10.1016/j.scitotenv.2017.01.066, 2017a.

Chen, J., Li, C., Ristovski, Z., Milic, A., Gu, Y., Islam, M. S., Wang, S., Hao, J., Zhang, H., He, C., Guo, H., Fu, H., Miljevic, B., Morawska, L., Thai, P., Lam, Y. F., Pereira, G., Ding, A., Huang, X., and Dumka, U. C.: A review of biomass burning: Emissions and impacts on air quality, health and climate in China, Sci. Total Environ., 579, 1000–1034, https://doi.org/10.1016/j.scitotenv.2016.11.025, 2017b.

Chen, R., Jiang, Y., Hu, J., Chen, H., Li, H., Meng, X., Ji, J. S., Gao, Y., Wang, W., Liu, C., Fang, W., Yan, H., Chen, J., Wang, W., Xiang, D., Su, X., Yu, B., Wang, Y., Xu, Y., Wang, L., Li, C., Chen, Y., Bell, M. L., Cohen, A. J., Ge, J., Huo, Y., and Kan, H.: Hourly Air Pollutants and Acute Coronary Syndrome Onset in 1.29 Million Patients, Circulation, 145, 1749–1760, https://doi.org/10.1161/CIRCULATIONAHA.121.057179, 2022.

Cheng, Y., Engling, G., He, K.-B., Duan, F.-K., Ma, Y.-L., Du, Z.-Y., Liu, J.-M., Zheng, M., and Weber, R. J.: Biomass burning contribution to Beijing aerosol, Atmos. Chem. Phys., 13, 7765–7781, https://doi.org/10.5194/acp-13-7765-2013, 2013.

Cheng, Y., Zheng, G., Wei, C., Mu, Q., Zheng, B., Wang, Z., Gao, M., Zhang, Q., He, K., Carmichael, G., Pöschl, U., and Su, H.: Reactive nitrogen chemistry in aerosol water as a source of sulfate during haze events in China, Sci. Adv., 2, e1601530, https://doi.org/10.1126/sciadv.1601530, 2016.

Claeys, M., Graham, B., Vas, G., Wang, W., Vermeylen, R., Pashynska, V., Cafmeyer, J., Guyon, P., Andreae, M. O., Artaxo, P., and Maenhaut, W.: Formation of Secondary Organic Aerosols Through Photooxidation of Isoprene, Science, 303, 1173–1176, https://doi.org/10.1126/science.1092805, 2004.

Claeys, M., Szmigielski, R., Kourtchev, I., Van der Veken, P., Vermeylen, R., Maenhaut, W., Jaoui, M., Kleindienst, T. E., Lewandowski, M., Offenberg, J. H., and Edney, E. O.: Hydroxydicarboxylic Acids: Markers for Secondary Organic Aerosol from the Photooxidation of á-Pinene, Environ. Sci. Technol., 41, 1628–1634, https://doi.org/10.1021/es0620181, 2007.

Ding, X., Zhang, Y.-Q., He, Q.-F., Yu, Q.-Q., Wang, J.-Q., Shen, R.-Q., Song, W., Wang, Y.-S., and Wang, X.-M.: Significant Increase of Aromatics-Derived Secondary Organic Aerosol during Fall to Winter in China, Environ. Sci. Technol., 51, 7432–7441, https://doi.org/10.1021/acs.est.6b06408, 2017.

Duhl, T. R., Helmig, D., and Guenther, A.: Sesquiterpene emissions from vegetation: a review, Biogeosciences, 5, 761–777, https://doi.org/10.5194/bg-5-761-2008, 2008.

Elias, V. O., Simoneit, B. R. T., Cordeiro, R. C., and Turcq, B.: Evaluating levoglucosan as an indicator of biomass burning in Carajás, amazônia: a comparison to the charcoal record2, Geochim. Cosmochim. Acta, 65, 267–272, https://doi.org/10.1016/S0016-7037(00)00522-6, 2001.

Fan, M.-Y., Zhang, Y.-L., Lin, Y.-C., Cao, F., Zhao, Z.-Y., Sun, Y., Qiu, Y., Fu, P., and Wang, Y.: Changes of Emission Sources to Nitrate Aerosols in Beijing After the Clean Air Actions: Evidence From Dual Isotope Compositions, J. Geophys. Res.-Atmos., 125, e2019JD031998, https://doi.org/10.1029/2019JD031998, 2020.

Fan, M.-Y., Zhang, W., Zhang, Y.-L., Li, J., Fang, H., Cao, F., Yan, M., Hong, Y., Guo, H., and Michalski, G.: Formation Mechanisms and Source Apportionments of Nitrate Aerosols in a Megacity of Eastern China Based On Multiple Isotope Observations, J. Geophys. Res.-Atmos., 128, e2022JD038129, https://doi.org/10.1029/2022JD038129, 2023.

Fine, P. M., Chakrabarti, B., Krudysz, M., Schauer, J. J., and Sioutas, C.: Diurnal Variations of Individual Organic Compound Constituents of Ultrafine and Accumulation Mode Particulate Matter in the Los Angeles Basin, Environ. Sci. Technol., 38, 1296–1304, https://doi.org/10.1021/es0348389, 2004.

Fu, P., Kawamura, K., Okuzawa, K., Aggarwal, S. G., Wang, G., Kanaya, Y., and Wang, Z.: Organic molecular compositions and temporal variations of summertime mountain aerosols over Mt. Tai, North China Plain, J. Geophys. Res.-Atmos., 113, D19107, https://doi.org/10.1029/2008JD009900, 2008.

Fu, P., Kawamura, K., Kanaya, Y., and Wang, Z.: Contributions of biogenic volatile organic compounds to the formation of secondary organic aerosols over Mt. Tai, Central East China, Atmos. Environ., 44, 4817–4826, https://doi.org/10.1016/j.atmosenv.2010.08.040, 2010.

Fu, P., Kawamura, K., Kobayashi, M., and Simoneit, B. R. T.: Seasonal variations of sugars in atmospheric particulate matter from Gosan, Jeju Island: Significant contributions of airborne pollen and Asian dust in spring, Atmos. Environ., 55, 234–239, https://doi.org/10.1016/j.atmosenv.2012.02.061, 2012.

Fu, P., Kawamura, K., Chen, J., and Miyazaki, Y.: Secondary production of organic aerosols from biogenic VOCs over Mt. Fuji, Japan, Environ. Sci. Technol., 48, 8491–8497, 2014.

Fu, P., Zhuang, G., Sun, Y., Wang, Q., Chen, J., Ren, L., Yang, F., Wang, Z., Pan, X., Li, X., and Kawamura, K.: Molecular markers of biomass burning, fungal spores and biogenic SOA

in the Taklimakan desert aerosols, Atmos. Environ., 130, 64–73, https://doi.org/10.1016/j.atmosenv.2015.10.087, 2016.

Gelencsér, A., May, B., Simpson, D., Sánchez-Ochoa, A., Kasper-Giebl, A., Puxbaum, H., Caseiro, A., Pio, C., and Legrand, M.: Source apportionment of $PM_{2.5}$ organic aerosol over Europe: Primary/secondary, natural/anthropogenic, and fossil/biogenic origin, J. Geophys. Res.-Atmos., 112, https://doi.org/10.1029/2006JD008094, 2007.

Gilardoni, S., Massoli, P., Paglione, M., Giulianelli, L., Carbone, C., Rinaldi, M., Decesari, S., Sandrini, S., Costabile, F., Gobbi, G. P., Pietrogrande, M. C., Visentin, M., Scotto, F., Fuzzi, S., and Facchini, M. C.: Direct observation of aqueous secondary organic aerosol from biomass-burning emissions, P. Natl. Acad. Sci. USA, 113, 10013–10018, https://doi.org/10.1073/pnas.1602212113, 2016.

Graham, B., Guyon, P., Taylor, P. E., Artaxo, P., Maenhaut, W., Glovsky, M. M., Flagan, R. C., and Andreae, M. O.: Organic compounds present in the natural Amazonian aerosol: Characterization by gas chromatography–mass spectrometry, J. Geophys. Res.-Atmos., 108, 4766, https://doi.org/10.1029/2003JD003990, 2003.

Griffin, R. J., Cocker III, D. R., Seinfeld, J. H., and Dabdub, D.: Estimate of global atmospheric organic aerosol from oxidation of biogenic hydrocarbons, Geophys. Res. Lett., 26, 2721–2724, https://doi.org/10.1029/1999GL900476, 1999.

Guenther, A., Karl, T., Harley, P., Wiedinmyer, C., Palmer, P. I., and Geron, C.: Estimates of global terrestrial isoprene emissions using MEGAN (Model of Emissions of Gases and Aerosols from Nature), Atmos. Chem. Phys., 6, 3181–3210, https://doi.org/10.5194/acp-6-3181-2006, 2006.

Hallquist, M., Wenger, J. C., Baltensperger, U., Rudich, Y., Simpson, D., Claeys, M., Dommen, J., Donahue, N. M., George, C., Goldstein, A. H., Hamilton, J. F., Herrmann, H., Hoffmann, T., Iinuma, Y., Jang, M., Jenkin, M. E., Jimenez, J. L., Kiendler-Scharr, A., Maenhaut, W., McFiggans, G., Mentel, Th. F., Monod, A., Prévôt, A. S. H., Seinfeld, J. H., Surratt, J. D., Szmigielski, R., and Wildt, J.: The formation, properties and impact of secondary organic aerosol: current and emerging issues, Atmos. Chem. Phys., 9, 5155–5236, https://doi.org/10.5194/acp-9-5155-2009, 2009.

Ho, K. F., Huang, R.-J., Kawamura, K., Tachibana, E., Lee, S. C., Ho, S. S. H., Zhu, T., and Tian, L.: Dicarboxylic acids, ketocarboxylic acids, α-dicarbonyls, fatty acids and benzoic acid in $PM_{2.5}$ aerosol collected during CAREBeijing-2007: an effect of traffic restriction on air quality, Atmos. Chem. Phys., 15, 3111–3123, https://doi.org/10.5194/acp-15-3111-2015, 2015.

Holden, A. S., Sullivan, A. P., Munchak, L. A., Kreidenweis, S. M., Schichtel, B. A., Malm, W. C., and Collett, J. L.: Determining contributions of biomass burning and other sources to fine particle contemporary carbon in the western United States, Atmos. Environ., 45, 1986–1993, https://doi.org/10.1016/j.atmosenv.2011.01.021, 2011.

Huang, R.-J., Zhang, Y., Bozzetti, C., Ho, K.-F., Cao, J.-J., Han, Y., Daellenbach, K. R., Slowik, J. G., Platt, S. M., Canonaco, F., Zotter, P., Wolf, R., Pieber, S. M., Bruns, E. A., Crippa, M., Ciarelli, G., Piazzalunga, A., Schwikowski, M., Abbaszade, G., Schnelle-Kreis, J., Zimmermann, R., An, Z., Szidat, S., Baltensperger, U., Haddad, I. E., and Prévôt, A. S. H.: High secondary aerosol contribution to particulate pollution during haze events in China, Nature, 514, 218–222, https://doi.org/10.1038/nature13774, 2014.

Huang, X., Ding, A., Wang, Z., Ding, K., Gao, J., Chai, F., and Fu, C.: Amplified transboundary transport of haze by aerosol–boundary layer interaction in China, Nat. Geosci., 13, 428–434, https://doi.org/10.1038/s41561-020-0583-4, 2020a.

Huang, X., Ding, A., Gao, J., Zheng, B., Zhou, D., Qi, X., Tang, R., Wang, J., Ren, C., Nie, W., Chi, X., Xu, Z., Chen, L., Li, Y., Che, F., Pang, N., Wang, H., Tong, D., Qin, W., Cheng, W., Liu, W., Fu, Q., Liu, B., Chai, F., Davis, S. J., Zhang, Q., and He, K.: Enhanced secondary pollution offset reduction of primary emissions during COVID-19 lockdown in China, Nat. Sci. Rev., 8, nwaa137, https://doi.org/10.1093/nsr/nwaa137, 2020b.

Jaoui, M., Lewandowski, M., Kleindienst, T. E., Offenberg, J. H., and Edney, E. O.: β-caryophyllinic acid: An atmospheric tracer for β-caryophyllene secondary organic aerosol, Geophys. Res. Lett., 34, L05816, https://doi.org/10.1029/2006GL028827, 2007.

Ji, D., Gao, W., Maenhaut, W., He, J., Wang, Z., Li, J., Du, W., Wang, L., Sun, Y., Xin, J., Hu, B., and Wang, Y.: Impact of air pollution control measures and regional transport on carbonaceous aerosols in fine particulate matter in urban Beijing, China: insights gained from long-term measurement, Atmos. Chem. Phys., 19, 8569–8590, https://doi.org/10.5194/acp-19-8569-2019, 2019.

Jia, Y. and Fraser, M.: Characterization of Saccharides in Size-fractionated Ambient Particulate Matter and Aerosol Sources: The Contribution of Primary Biological Aerosol Particles (PBAPs) and Soil to Ambient Particulate Matter, Environ. Sci. Technol., 45, 930–936, https://doi.org/10.1021/es103104e, 2011.

Jimenez, J. L., Canagaratna, M. R., Donahue, N. M., Prevot, A. S. H., Zhang, Q., Kroll, J. H., DeCarlo, P. F., Allan, J. D., Coe, H., Ng, N. L., Aiken, A. C., Docherty, K. S., Ulbrich, I. M., Grieshop, A. P., Robinson, A. L., Duplissy, J., Smith, J. D., Wilson, K. R., Lanz, V. A., Hueglin, C., Sun, Y. L., Tian, J., Laaksonen, A., Raatikainen, T., Rautiainen, J., Vaattovaara, P., Ehn, M., Kulmala, M., Tomlinson, J. M., Collins, D. R., Cubison, M. J., E., Dunlea, J., Huffman, J. A., Onasch, T. B., Alfarra, M. R., Williams, P. I., Bower, K., Kondo, Y., Schneider, J., Drewnick, F., Borrmann, S., Weimer, S., Demerjian, K., Salcedo, D., Cottrell, L., Griffin, R., Takami, A., Miyoshi, T., Hatakeyama, S., Shimono, A., Sun, J. Y., Zhang, Y. M., Dzepina, K., Kimmel, J. R., Sueper, D., Jayne, J. T., Herndon, S. C., Trimborn, A. M., Williams, L. R., Wood, E. C., Middlebrook, A. M., Kolb, C. E., Baltensperger, U., and Worsnop, D. R.: Evolution of Organic Aerosols in the Atmosphere, Science, 326, 1525–1529, https://doi.org/10.1126/science.1180353, 2009.

Kanakidou, M., Seinfeld, J. H., Pandis, S. N., Barnes, I., Dentener, F. J., Facchini, M. C., Van Dingenen, R., Ervens, B., Nenes, A., Nielsen, C. J., Swietlicki, E., Putaud, J. P., Balkanski, Y., Fuzzi, S., Horth, J., Moortgat, G. K., Winterhalter, R., Myhre, C. E. L., Tsigaridis, K., Vignati, E., Stephanou, E. G., and Wilson, J.: Organic aerosol and global climate modelling: a review, Atmos. Chem. Phys., 5, 1053–1123, https://doi.org/10.5194/acp-5-1053-2005, 2005.

Kang, M., Fu, P., Aggarwal, S. G., Kumar, S., Zhao, Y., Sun, Y., and Wang, Z.: Size distributions of n-alkanes, fatty acids and fatty alcohols in springtime aerosols from New Delhi, India, Environ. Pollut., 219, 957–966, https://doi.org/10.1016/j.envpol.2016.09.077, 2016.

Kang, M., Fu, P., Kawamura, K., Yang, F., Zhang, H., Zang, Z., Ren, H., Ren, L., Zhao, Y., Sun, Y., and Wang, Z.: Characterization of biogenic primary and secondary organic aerosols in the marine atmosphere over the East China Sea, Atmos. Chem. Phys., 18, 13947–13967, https://doi.org/10.5194/acp-18-13947-2018, 2018a.

Kang, M., Ren, L., Ren, H., Zhao, Y., Kawamura, K., Zhang, H., Wei, L., Sun, Y., Wang, Z., and Fu, P.: Primary biogenic and anthropogenic sources of organic aerosols in Beijing, China: Insights from saccharides and n-alkanes, Environ. Pollut., 243, 1579–1587, https://doi.org/10.1016/j.envpol.2018.09.118, 2018b.

Kang, M., Guo, H., Wang, P., Fu, P., Ying, Q., Liu, H., Zhao, Y., and Zhang, H.: Characterization and source apportionment of marine aerosols over the East China Sea, Sci. Total Environ., 651, 2679–2688, https://doi.org/10.1016/j.scitotenv.2018.10.174, 2019.

Kang, M., Zhang, J., Zhang, H., and Ying, Q.: On the Relevancy of Observed Ozone Increase during COVID-19 Lockdown to Summertime Ozone and $PM_{2.5}$ Control Policies in China, Environ. Sci. Technol. Lett., 8, 289–294, https://doi.org/10.1021/acs.estlett.1c00036, 2021.

Kaufman, Y. J., Tanré, D., and Boucher, O.: A satellite view of aerosols in the climate system, Nature, 419, 215–223, https://doi.org/10.1038/nature01091, 2002.

Kawamura, K. and Sakaguchi, F.: Molecular distributions of water soluble dicarboxylic acids in marine aerosols over the Pacific Ocean including tropics, J. Geophys. Res.-Atmos., 104, 3501–3509, https://doi.org/10.1029/1998JD100041, 1999.

Kawana, K., Miyazaki, Y., Omori, Y., Tanimoto, H., Kagami, S., Suzuki, K., Yamashita, Y., Nishioka, J., Deng, Y., Yai, H., and Mochida, M.: Number-Size Distribution and CCN Activity of Atmospheric Aerosols in the Western North Pacific During Spring Pre-Bloom Period: Influences of Terrestrial and Marine Sources, J. Geophys. Res.-Atmos., 127, e2022JD036690, https://doi.org/10.1029/2022JD036690, 2022.

Kleindienst, T. E., Jaoui, M., Lewandowski, M., Offenberg, J. H., Lewis, C. W., Bhave, P. V., and Edney, E. O.: Estimates of the contributions of biogenic and anthropogenic hydrocarbons to secondary organic aerosol at a southeastern US location, Atmos. Environ., 41, 8288–8300, https://doi.org/10.1016/j.atmosenv.2007.06.045, 2007.

Kleindienst, T. E., Jaoui, M., Lewandowski, M., Offenberg, J. H., and Docherty, K. S.: The formation of SOA and chemical tracer compounds from the photooxidation of naphthalene and its methyl analogs in the presence and absence of nitrogen oxides, Atmos. Chem. Phys., 12, 8711–8726, https://doi.org/10.5194/acp-12-8711-2012, 2012.

Le, T., Wang, Y., Liu, L., Yang, J., Yung, Y. L., Li, G., and Seinfeld, J. H.: Unexpected air pollution with marked emission reductions during the COVID-19 outbreak in China, Science, 369, 702–706, https://doi.org/10.1126/science.abb7431, 2020.

Li, B., Zhang, J., Zhao, Y., Yuan, S., Zhao, Q., Shen, G., and Wu, H.: Seasonal variation of urban carbonaceous aerosols in a typical city Nanjing in Yangtze River Delta, China, Atmos. Environ., 106, 223–231, https://doi.org/10.1016/j.atmosenv.2015.01.064, 2015.

Li, C., Bosch, C., Kang, S., Andersson, A., Chen, P., Zhang, Q., Cong, Z., Chen, B., Qin, D., and Gustafsson, Ö.: Sources of black carbon to the Himalayan–Tibetan Plateau glaciers, Nat. Commun., 7, 12574, https://doi.org/10.1038/ncomms12574, 2016a.

Li, F., Tsona, N. T., Li, J., and Du, L.: Aqueous-phase oxidation of syringic acid emitted from biomass burning: Formation of light-absorbing compounds, Sci. Total Environ., 765, 144239, https://doi.org/10.1016/j.scitotenv.2020.144239, 2021a.

Li, H., Wang, Q., Yang, M., Li, F., Wang, J., Sun, Y., Wang, C., Wu, H., and Qian, X.: Chemical characterization and source apportionment of $PM_{2.5}$ aerosols in a megacity of Southeast China, Atmos. Res., 181, 288–299, https://doi.org/10.1016/j.atmosres.2016.07.005, 2016b.

Li, J. J., Wang, G. H., Cao, J. J., Wang, X. M., and Zhang, R. J.: Observation of biogenic secondary organic aerosols in the atmosphere of a mountain site in central China: temperature and relative humidity effects, Atmos. Chem. Phys., 13, 11535–11549, https://doi.org/10.5194/acp-13-11535-2013, 2013.

Li, K., Zhang, J., Bell, D. M., Wang, T., Lamkaddam, H., Cui, T., Qi, L., Surdu, M., Wang, D., Du, L., El Haddad, I., Slowik, J. G., and Prevot, A. S. H.: Uncovering the dominant contribution of intermediate volatility compounds in secondary organic aerosol formation from biomass-burning emissions, Nat. Sci. Rev., 11, nwae014, https://doi.org/10.1093/nsr/nwae014, 2024.

Li, L., Ren, L., Ren, H., Yue, S., Xie, Q., Zhao, W., Kang, M., Li, J., Wang, Z., Sun, Y., and Fu, P.: Molecular Characterization and Seasonal Variation in Primary and Secondary Organic Aerosols in Beijing, China, J. Geophys. Res.-Atmos., 123, 12394–12412, https://doi.org/10.1029/2018JD028527, 2018.

Li, X.-B., Yuan, B., Wang, S., Wang, C., Lan, J., Liu, Z., Song, Y., He, X., Huangfu, Y., Pei, C., Cheng, P., Yang, S., Qi, J., Wu, C., Huang, S., You, Y., Chang, M., Zheng, H., Yang, W., Wang, X., and Shao, M.: Variations and sources of volatile organic compounds (VOCs) in urban region: insights from measurements on a tall tower, Atmos. Chem. Phys., 22, 10567–10587, https://doi.org/10.5194/acp-22-10567-2022, 2022.

Li, Y., Fu, T.-M., Yu, J. Z., Feng, X., Zhang, L., Chen, J., Boreddy, S. K. R., Kawamura, K., Fu, P., Yang, X., Zhu, L., and Zeng, Z.: Impacts of Chemical Degradation on the Global Budget of Atmospheric Levoglucosan and Its Use As a Biomass Burning Tracer, Environ. Sci. Technol., 55, 5525–5536, https://doi.org/10.1021/acs.est.0c07313, 2021b.

Li, Y. J., Huang, D. D., Cheung, H. Y., Lee, A. K. Y., and Chan, C. K.: Aqueous-phase photochemical oxidation and direct photolysis of vanillin – a model compound of methoxy phenols from biomass burning, Atmos. Chem. Phys., 14, 2871–2885, https://doi.org/10.5194/acp-14-2871-2014, 2014.

Lim, C. Y., Hagan, D. H., Coggon, M. M., Koss, A. R., Sekimoto, K., de Gouw, J., Warneke, C., Cappa, C. D., and Kroll, J. H.: Secondary organic aerosol formation from the laboratory oxidation of biomass burning emissions, Atmos. Chem. Phys., 19, 12797–12809, https://doi.org/10.5194/acp-19-12797-2019, 2019.

Lin, Y.-C., Zhang, Y.-L., Fan, M.-Y., and Bao, M.: Heterogeneous formation of particulate nitrate under ammonium-rich regimes during the high-$PM_{2.5}$ events in Nanjing, China, Atmos. Chem. Phys., 20, 3999–4011, https://doi.org/10.5194/acp-20-3999-2020, 2020.

Lin, Y.-C., Fan, M.-Y., Hong, Y., Yu, M., Cao, F., and Zhang, Y.-L.: Important contributions of natural gas combustion to atmospheric nitrate aerosols in China: Insights

from stable nitrogen isotopes, Sci. Bull., 69, 3001–3004, https://doi.org/10.1016/j.scib.2024.06.038, 2024.

Lin, Y.-H., Zhang, H., Pye, H. O. T., Zhang, Z., Marth, W. J., Park, S., Arashiro, M., Cui, T., Budisulistiorini, S. H., Sexton, K. G., Vizuete, W., Xie, Y., Luecken, D. J., Piletic, I. R., Edney, E. O., Bartolotti, L. J., Gold, A., and Surratt, J. D.: Epoxide as a precursor to secondary organic aerosol formation from isoprene photooxidation in the presence of nitrogen oxides, P. Natl. Acad. Sci. USA, 110, 6718–6723, https://doi.org/10.1073/pnas.1221150110, 2013a.

Lin, Y.-H., Knipping, E. M., Edgerton, E. S., Shaw, S. L., and Surratt, J. D.: Investigating the influences of SO_2 and NH_3 levels on isoprene-derived secondary organic aerosol formation using conditional sampling approaches, Atmos. Chem. Phys., 13, 8457–8470, https://doi.org/10.5194/acp-13-8457-2013, 2013b.

Liu, D., Li, J., Zhang, Y., Xu, Y., Liu, X., Ding, P., Shen, C., Chen, Y., Tian, C., and Zhang, G.: The Use of Levoglucosan and Radiocarbon for Source Apportionment of $PM_{2.5}$ Carbonaceous Aerosols at a Background Site in East China, Environ. Sci. Technol., 47, 10454–10461, https://doi.org/10.1021/es401250k, 2013.

Liu, J., Li, J., Zhang, Y., Liu, D., Ding, P., Shen, C., Shen, K., He, Q., Ding, X., Wang, X., Chen, D., Szidat, S., and Zhang, G.: Source Apportionment Using Radiocarbon and Organic Tracers for $PM_{2.5}$ Carbonaceous Aerosols in Guangzhou, South China: Contrasting Local- and Regional-Scale Haze Events, Environ. Sci. Technol., 48, 12002–12011, https://doi.org/10.1021/es503102w, 2014.

Liu, J., Li, J., Liu, D., Ding, P., Shen, C., Mo, Y., Wang, X., Luo, C., Cheng, Z., Szidat, S., Zhang, Y., Chen, Y., and Zhang, G.: Source apportionment and dynamic changes of carbonaceous aerosols during the haze bloom-decay process in China based on radiocarbon and organic molecular tracers, Atmos. Chem. Phys., 16, 2985–2996, https://doi.org/10.5194/acp-16-2985-2016, 2016.

Lu, K., Guo, S., Tan, Z., Wang, H., Shang, D., Liu, Y., Li, X., Wu, Z., Hu, M., and Zhang, Y.: Exploring atmospheric free-radical chemistry in China: the self-cleansing capacity and the formation of secondary air pollution, Nat. Sci. Rev., 6, 579–594, https://doi.org/10.1093/nsr/nwy073, 2019.

Medeiros, P. M., Conte, M. H., Weber, J. C., and Simoneit, B. R. T.: Sugars as source indicators of biogenic organic carbon in aerosols collected above the Howland Experimental Forest, Maine, Atmos. Environ., 40, 1694–1705, https://doi.org/10.1016/j.atmosenv.2005.11.001, 2006.

Mochida, M., Kawamura, K., Fu, P., and Takemura, T.: Seasonal variation of levoglucosan in aerosols over the western North Pacific and its assessment as a biomass-burning tracer, Atmos. Environ., 44, 3511–3518, https://doi.org/10.1016/j.atmosenv.2010.06.017, 2010.

Morris, C. E., Sands, D. C., Bardin, M., Jaenicke, R., Vogel, B., Leyronas, C., Ariya, P. A., and Psenner, R.: Microbiology and atmospheric processes: research challenges concerning the impact of airborne micro-organisms on the atmosphere and climate, Biogeosciences, 8, 17–25, https://doi.org/10.5194/bg-8-17-2011, 2011.

Mozaffar, A., Zhang, Y.-L., Fan, M., Cao, F., and Lin, Y.-C.: Characteristics of summertime ambient VOCs and their contributions to O_3 and SOA formation in a sub-urban area of Nanjing, China, Atmos. Res., 240, 104923, https://doi.org/10.1016/j.atmosres.2020.104923, 2020.

Pope, C. A., Burnett, R. T., Thurston, G. D., Thun, M. J., Calle, E. E., Krewski, D., and Godleski, J. J.: Cardiovascular Mortality and Long-Term Exposure to Particulate Air Pollution, Circulation, 109, 71–77, https://doi.org/10.1161/01.CIR.0000108927.80044.7F, 2004.

Pöschl, U., Martin, S. T., Sinha, B., Chen, Q., Gunthe, S. S., Huffman, J. A., Borrmann, S., Farmer, D. K., Garland, R. M., Helas, G., Jimenez, J. L., King, S. M., Manzi, A., Mikhailov, E., Pauliquevis, T., Petters, M. D., Prenni, A. J., Roldin, P., Rose, D., Schneider, J., Su, H., Zorn, S. R., Artaxo, P., and Andreae, M. O.: Rainforest Aerosols as Biogenic Nuclei of Clouds and Precipitation in the Amazon, Science, 329, 1513–1516, https://doi.org/10.1126/science.1191056, 2010.

Puxbaum, H. and Tenze-Kunit, M.: Size distribution and seasonal variation of atmospheric cellulose, Atmos. Environ., 37, 3693–3699, https://doi.org/10.1016/S1352-2310(03)00451-5, 2003.

Ram, K., Sarin, M. M., and Hegde, P.: Long-term record of aerosol optical properties and chemical composition from a high-altitude site (Manora Peak) in Central Himalaya, Atmos. Chem. Phys., 10, 11791–11803, https://doi.org/10.5194/acp-10-11791-2010, 2010.

Ren, G., Yan, X., Ma, Y., Qiao, L., Chen, Z., Xin, Y., Zhou, M., Shi, Y., Zheng, K., Zhu, S., Huang, C., and Li, L.: Characteristics and source apportionment of $PM_{2.5}$-bound saccharides and carboxylic acids in Central Shanghai, China, Atmos. Res., 237, 104817, https://doi.org/10.1016/j.atmosres.2019.104817, 2020.

Rivellini, L.-H., Jorga, S., Wang, Y., Lee, A. K. Y., Murphy, J. G., Chan, A. W., and Abbatt, J. P. D.: Sources of Wintertime Atmospheric Organic Pollutants in a Large Canadian City: Insights from Particle and Gas Phase Measurements, ACS EST Air, https://doi.org/10.1021/acsestair.4c00039, 2024.

Rogge, W. F., Hildemann, L. M., Mazurek, M. A., Cass, G. R., and Simoneit, B. R. T.: Sources of fine organic aerosol. 2. Noncatalyst and catalyst-equipped automobiles and heavy-duty diesel trucks, Environ. Sci. Technol., 27, 636–651, https://doi.org/10.1021/es00041a007, 1993.

Rogge, W. F., Medeiros, P. M., and Simoneit, B. R. T.: Organic marker compounds in surface soils of crop fields from the San Joaquin Valley fugitive dust characterization study, Atmos. Environ., 41, 8183–8204, https://doi.org/10.1016/j.atmosenv.2007.06.030, 2007.

Shah, V., Keller, C. A., Knowland, K. E., Christiansen, A., Hu, L., Wang, H., Lu, X., Alexander, B., and Jacob, D. J.: Particulate Nitrate Photolysis as a Possible Driver of Rising Tropospheric Ozone, Geophys. Res. Lett., 51, e2023GL107980, https://doi.org/10.1029/2023GL107980, 2024.

Sharkey, T. D., Wiberley, A. E., and Donohue, A. R.: Isoprene Emission from Plants: Why and How, Ann. Bot., 101, 5–18, https://doi.org/10.1093/aob/mcm240, 2008.

Simoneit, B. R. T.: Biomass burning – a review of organic tracers for smoke from incomplete combustion, Appl. Geochem., 17, 129–162, https://doi.org/10.1016/S0883-2927(01)00061-0, 2002.

Simoneit, B. R. T., Kobayashi, M., Mochida, M., Kawamura, K., and Huebert, B. J.: Aerosol particles collected on aircraft flights over the northwestern Pacific region during the ACE-Asia campaign: Composition and major sources of the

organic compounds, J. Geophys. Res.-Atmos., 109, D19S09, https://doi.org/10.1029/2004JD004565, 2004a.

Simoneit, B. R. T., Elias, V. O., Kobayashi, M., Kawamura, K., Rushdi, A. I., Medeiros, P. M., Rogge, W. F., and Didyk, B. M.: SugarsDominant Water-Soluble Organic Compounds in Soils and Characterization as Tracers in Atmospheric Particulate Matter, Environ. Sci. Technol., 38, 5939–5949, https://doi.org/10.1021/es0403099, 2004b.

Sindelarova, K., Granier, C., Bouarar, I., Guenther, A., Tilmes, S., Stavrakou, T., Müller, J.-F., Kuhn, U., Stefani, P., and Knorr, W.: Global data set of biogenic VOC emissions calculated by the MEGAN model over the last 30 years, Atmos. Chem. Phys., 14, 9317–9341, https://doi.org/10.5194/acp-14-9317-2014, 2014.

Song, W., Zhang, Y.-L., Zhang, Y., Cao, F., Rauber, M., Salazar, G., Kawichai, S., Prapamontol, T., and Szidat, S.: Is biomass burning always a dominant contributor of fine aerosols in upper northern Thailand?, Environ. Int., 168, 107466, https://doi.org/10.1016/j.envint.2022.107466, 2022.

Srivastava, D., Vu, T. V., Tong, S., Shi, Z., and Harrison, R. M.: Formation of secondary organic aerosols from anthropogenic precursors in laboratory studies, npj Clim. Atmos. Sci., 5, 1–30, https://doi.org/10.1038/s41612-022-00238-6, 2022.

Suh, I., Zhang, R., Molina, L. T., and Molina, M. J.: Oxidation Mechanism of Aromatic Peroxy and Bicyclic Radicals from OH-Toluene Reactions, J. Am. Chem. Soc., 125, 12655–12665, https://doi.org/10.1021/ja0350280, 2003.

Sullivan, A. P., Holden, A. S., Patterson, L. A., McMeeking, G. R., Kreidenweis, S. M., Malm, W. C., Hao, W. M., Wold, C. E., and Collett Jr., J. L.: A method for smoke marker measurements and its potential application for determining the contribution of biomass burning from wildfires and prescribed fires to ambient $PM_{2.5}$ organic carbon, J. Geophys. Res.-Atmos., 113, D22302, https://doi.org/10.1029/2008JD010216, 2008.

Sun, Y., Jiang, Q., Wang, Z., Fu, P., Li, J., Yang, T., and Yin, Y.: Investigation of the sources and evolution processes of severe haze pollution in Beijing in January 2013, J. Geophys. Res.-Atmos., 119, 4380–4398, https://doi.org/10.1002/2014JD021641, 2014.

Surratt, J. D., Murphy, S. M., Kroll, J. H., Ng, N. L., Hildebrandt, L., Sorooshian, A., Szmigielski, R., Vermeylen, R., Maenhaut, W., Claeys, M., Flagan, R. C., and Seinfeld, J. H.: Chemical Composition of Secondary Organic Aerosol Formed from the Photooxidation of Isoprene, J. Phys. Chem. A, 110, 9665–9690, https://doi.org/10.1021/jp061734m, 2006.

Surratt, J. D., Chan, A. W. H., Eddingsaas, N. C., Chan, M., Loza, C. L., Kwan, A. J., Hersey, S. P., Flagan, R. C., Wennberg, P. O., and Seinfeld, J. H.: Reactive intermediates revealed in secondary organic aerosol formation from isoprene, P. Natl. Acad. Sci. USA, 107, 6640–6645, https://doi.org/10.1073/pnas.0911114107, 2010.

Turpin, B. J. and Lim, H.-J.: Species Contributions to PM2.5 Mass Concentrations: Revisiting Common Assumptions for Estimating Organic Mass, Aerosol Sci. Technol., 35, 602–610, https://doi.org/10.1080/02786820119445, 2001.

Urban, R. C., Lima-Souza, M., Caetano-Silva, L., Queiroz, M. E. C., Nogueira, R. F. P., Allen, A. G., Cardoso, A. A., Held, G., and Campos, M. L. A. M.: Use of levoglucosan, potassium, and water-soluble organic carbon to characterize the origins of biomass-burning aerosols, Atmos. Environ., 61, 562–569, https://doi.org/10.1016/j.atmosenv.2012.07.082, 2012.

Virkkula, A., Teinilä, K., Hillamo, R., Kerminen, V.-M., Saarikoski, S., Aurela, M., Viidanoja, J., Paatero, J., Koponen, I. K., and Kulmala, M.: Chemical composition of boundary layer aerosol over the Atlantic Ocean and at an Antarctic site, Atmos. Chem. Phys., 6, 3407–3421, https://doi.org/10.5194/acp-6-3407-2006, 2006.

Wang, G., Kawamura, K., Lee, S., Ho, K., and Cao, J.: Molecular, Seasonal, and Spatial Distributions of Organic Aerosols from Fourteen Chinese Cities, Environ. Sci. Technol., 40, 4619–4625, https://doi.org/10.1021/es060291x, 2006.

Wang, L., Li, Q., Qiu, Q., Hou, L., Ouyang, J., Zeng, R., Huang, S., Li, J., Tang, L., and Liu, Y.: Assessing the ecological risk induced by $PM_{2.5}$ pollution in a fast developing urban agglomeration of southeastern China, J. Environ. Manage., 324, 116284, https://doi.org/10.1016/j.jenvman.2022.116284, 2022.

Wang, P., Chen, K., Zhu, S., Wang, P., and Zhang, H.: Severe air pollution events not avoided by reduced anthropogenic activities during COVID-19 outbreak, Resour. Conserv. Recy., 158, 104814, https://doi.org/10.1016/j.resconrec.2020.104814, 2020.

Wu, X., Cao, F., Haque, M., Fan, M.-Y., Zhang, S.-C., and Zhang, Y.-L.: Molecular composition and source apportionment of fine organic aerosols in Northeast China, Atmos. Environ., 239, 117722, https://doi.org/10.1016/j.atmosenv.2020.117722, 2020.

Xiao, Y., Hu, M., Li, X., Zong, T., Xu, N., Hu, S., Zeng, L., Chen, S., Song, Y., Guo, S., and Wu, Z.: Aqueous secondary organic aerosol formation attributed to phenols from biomass burning, Sci. Total Environ., 847, 157582, https://doi.org/10.1016/j.scitotenv.2022.157582, 2022.

Yan, C., Tham, Y. J., Nie, W., Xia, M., Wang, H., Guo, Y., Ma, W., Zhan, J., Hua, C., Li, Y., Deng, C., Li, Y., Zheng, F., Chen, X., Li, Q., Zhang, G., Mahajan, A. S., Cuevas, C. A., Huang, D. D., Wang, Z., Sun, Y., Saiz-Lopez, A., Bianchi, F., Kerminen, V.-M., Worsnop, D. R., Donahue, N. M., Jiang, J., Liu, Y., Ding, A., and Kulmala, M.: Increasing contribution of nighttime nitrogen chemistry to wintertime haze formation in Beijing observed during COVID-19 lockdowns, Nat. Geosci., 16, 975–981, https://doi.org/10.1038/s41561-023-01285-1, 2023.

Yang, G.-P., Zhang, S.-H., Zhang, H.-H., Yang, J., and Liu, C.-Y.: Distribution of biogenic sulfur in the Bohai Sea and northern Yellow Sea and its contribution to atmospheric sulfate aerosol in the late fall, Mar. Chem., 169, 23–32, https://doi.org/10.1016/j.marchem.2014.12.008, 2015.

Yang, T., Li, H., Xu, W., Song, Y., Xu, L., Wang, H., Wang, F., Sun, Y., Wang, Z., and Fu, P.: Strong Impacts of Regional Atmospheric Transport on the Vertical Distribution of Aerosol Ammonium over Beijing, Environ. Sci. Technol. Lett., 11, 29–34, https://doi.org/10.1021/acs.estlett.3c00791, 2024.

Yang, Y., Chan, C., Tao, J., Lin, M., Engling, G., Zhang, Z., Zhang, T., and Su, L.: Observation of elevated fungal tracers due to biomass burning in the Sichuan Basin at Chengdu City, China, Sci. Total Environ., 431, 68–77, https://doi.org/10.1016/j.scitotenv.2012.05.033, 2012.

Yee, L. D., Kautzman, K. E., Loza, C. L., Schilling, K. A., Coggon, M. M., Chhabra, P. S., Chan, M. N., Chan, A. W. H., Hersey, S. P., Crounse, J. D., Wennberg, P. O., Flagan, R. C., and Seinfeld, J. H.: Secondary organic aerosol formation from biomass burning intermediates: phenol and methoxyphenols, Atmos. Chem. Phys., 13, 8019–8043, https://doi.org/10.5194/acp-13-8019-2013, 2013.

Youn, J.-S., Wang, Z., Wonaschütz, A., Arellano, A., Betterton, E. A., and Sorooshian, A.: Evidence of aqueous secondary organic aerosol formation from biogenic emissions in the North American Sonoran Desert, Geophys. Res. Lett., 40, 3468–3472, https://doi.org/10.1002/grl.50644, 2013.

Zhang, H., Li, J., Ying, Q., Yu, J. Z., Wu, D., Cheng, Y., He, K., and Jiang, J.: Source apportionment of $PM_{2.5}$ nitrate and sulfate in China using a source-oriented chemical transport model, Atmos. Environ., 62, 228–242, https://doi.org/10.1016/j.atmosenv.2012.08.014, 2012.

Zhang, H., Hu, J., Kleeman, M., and Ying, Q.: Source apportionment of sulfate and nitrate particulate matter in the Eastern United States and effectiveness of emission control programs, Sci. Total Environ., 490, 171–181, https://doi.org/10.1016/j.scitotenv.2014.04.064, 2014a.

Zhang, J., He, X., Ding, X., Yu, J. Z., and Ying, Q.: Modeling Secondary Organic Aerosol Tracers and Tracer-to-SOA Ratios for Monoterpenes and Sesquiterpenes Using a Chemical Transport Model, Environ. Sci. Technol., 56, 804–813, https://doi.org/10.1021/acs.est.1c06373, 2022.

Zhang, J., Liu, J., Ding, X., He, X., Zhang, T., Zheng, M., Choi, M., Isaacman-VanWertz, G., Yee, L., Zhang, H., Misztal, P., Goldstein, A. H., Guenther, A. B., Budisulistiorini, S. H., Surratt, J. D., Stone, E. A., Shrivastava, M., Wu, D., Yu, J. Z., and Ying, Q.: New formation and fate of Isoprene SOA markers revealed by field data-constrained modeling, npj Clim. Atmos. Sci., 6, 1–8, https://doi.org/10.1038/s41612-023-00394-3, 2023.

Zhang, J., Shrivastava, M., Ma, L., Jiang, W., Anastasio, C., Zhang, Q., and Zelenyuk, A.: Modeling Novel Aqueous Particle and Cloud Chemistry Processes of Biomass Burning Phenols and Their Potential to Form Secondary Organic Aerosols, Environ. Sci. Technol., 58, 3776–3786, https://doi.org/10.1021/acs.est.3c07762, 2024.

Zhang, T., Claeys, M., Cachier, H., Dong, S., Wang, W., Maenhaut, W., and Liu, X.: Identification and estimation of the biomass burning contribution to Beijing aerosol using levoglucosan as a molecular marker, Atmos. Environ., 42, 7013–7021, https://doi.org/10.1016/j.atmosenv.2008.04.050, 2008.

Zhang, Y., Huang, J.-P., Henze, D. K., and Seinfeld, J. H.: Role of isoprene in secondary organic aerosol formation on a regional scale, J. Geophys. Res.-Atmos., 112, D20207, https://doi.org/10.1029/2007JD008675, 2007.

Zhang, Y., Ren, H., Sun, Y., Cao, F., Chang, Y., Liu, S., Lee, X., Agrios, K., Kawamura, K., Liu, D., Ren, L., Du, W., Wang, Z., Prévôt, A. S. H., Szidat, S., and Fu, P.: High Contribution of Nonfossil Sources to Submicrometer Organic Aerosols in Beijing, China, Environ. Sci. Technol., 51, 7842–7852, https://doi.org/10.1021/acs.est.7b01517, 2017.

Zhang, Y.-L., Li, J., Zhang, G., Zotter, P., Huang, R.-J., Tang, J.-H., Wacker, L., Prévôt, A. S. H., and Szidat, S.: Radiocarbon-Based Source Apportionment of Carbonaceous Aerosols at a Regional Background Site on Hainan Island, South China, Environ. Sci. Technol., 48, 2651–2659, https://doi.org/10.1021/es4050852, 2014b.

Zhang, Y.-L., Huang, R.-J., El Haddad, I., Ho, K.-F., Cao, J.-J., Han, Y., Zotter, P., Bozzetti, C., Daellenbach, K. R., Canonaco, F., Slowik, J. G., Salazar, G., Schwikowski, M., Schnelle-Kreis, J., Abbaszade, G., Zimmermann, R., Baltensperger, U., Prévôt, A. S. H., and Szidat, S.: Fossil vs. non-fossil sources of fine carbonaceous aerosols in four Chinese cities during the extreme winter haze episode of 2013, Atmos. Chem. Phys., 15, 1299–1312, https://doi.org/10.5194/acp-15-1299-2015, 2015.

Zhang, Y.-L., Kawamura, K., Agrios, K., Lee, M., Salazar, G., and Szidat, S.: Fossil and Nonfossil Sources of Organic and Elemental Carbon Aerosols in the Outflow from Northeast China, Environ. Sci. Technol., 50, 6284–6292, https://doi.org/10.1021/acs.est.6b00351, 2016.

Zhang, Y.-L., El-Haddad, I., Huang, R.-J., Ho, K.-F., Cao, J.-J., Han, Y., Zotter, P., Bozzetti, C., Daellenbach, K. R., Slowik, J. G., Salazar, G., Prévôt, A. S. H., and Szidat, S.: Large contribution of fossil fuel derived secondary organic carbon to water soluble organic aerosols in winter haze in China, Atmos. Chem. Phys., 18, 4005–4017, https://doi.org/10.5194/acp-18-4005-2018, 2018.

Zhu, C., Kawamura, K., and Kunwar, B.: Effect of biomass burning over the western North Pacific Rim: wintertime maxima of anhydrosugars in ambient aerosols from Okinawa, Atmos. Chem. Phys., 15, 1959–1973, https://doi.org/10.5194/acp-15-1959-2015, 2015a.

Zhu, C., Kawamura, K., and Kunwar, B.: Organic tracers of primary biological aerosol particles at subtropical Okinawa Island in the western North Pacific Rim, J. Geophys. Res.-Atmos., 120, 5504–5523, https://doi.org/10.1002/2015JD023611, 2015b.